M.TECH DISSERTATION REPORT

ON

Failure Analysis & Improvement of Ti6Al4V Dental Implant

BY

ARVIND KUMAR VERMA

(2015PDE5090)

UNDER THE SUPERVISION OF

DR. AMIT SINGH

DEPARTMENT OF MECHANICAL ENGINEERING,

MALAVIYA NATIONAL INSTITUE OF TECHNOLOGY,

JAIPUR-302017 (RAJASTHAN).

2016-2017

A

DISSERTATION REPORT

ON

"Failure Analysis & Improvement of Ti6Al4V Dental Implant"

Submitted in partial fulfillment of the requirements for the award of degree of

MASTER OF TECHNOLOGY

IN

DESIGN ENGINEERING

Submitted by

Arvind Kumar Verma

(2015pde5090)

Supervised by

Dr. Amit Singh

(Assistant Professor)

DEPARTMENT OF MECHANICAL ENGINEERING,

MALAVIYA NATIONAL INSTITUTE OF TECHNOLOGY,

JAIPUR-302017 (RAJASTHAN).

2016-2017

© Malaviya National Institute of Technology Jaipur – 2016

All rights reserved

DEPARTMENT OF MECHANICAL ENGINEERING,

MALAVIYA NATIONAL INSTITUTE OF TECHNOLOGY,

JAIPUR-302017 (RAJASTHAN).

CERTIFICATE

This is to certify that the dissertation work entitled "Failure Analysis & Improvement of Ti6Al4V Dental Implant" by Mr. Arvind Kumar Verma is a bonafide work completed under my supervision and guidance, and hence approved for submission to the Department of Mechanical Engineering, Malaviya National Institute of Technology in partial fulfillment of the requirements for the award of the degree of Master of Technology with specialization in Design Engineering. The matter embodied in this Seminar Report has not been submitted for the award of any other degree, or diploma.

Place: Jaipur **Dr. Amit Singh**

Date: / / **(Assistant professor)**

DEPARTMENT OF MECHANICAL ENGINEERING,

MALAVIYA NATIONAL INSTITUTE OF TECHNOLOGY,

JAIPUR-302017 (RAJASTHAN).

Candidate's Declaration

I hereby certify that the work which is being presented in the dissertation entitled"Failure Analysis & Improvement of Ti6Al4V Dental Implant", in partial fulfilment of the requirements for the award of the Degree of Master of Technology in Design Engineering, submitted in the Department of Mechanical Engineering, MNIT, Jaipur is an authentic record of my own work carried out for a period of one year under the supervision of Dr. Amit Singh, Assistant professor of Mechanical Engineering Department, MNIT, Jaipur.

I have not submitted the matter embodied in this dissertation for the award of any other degree.

Place: Jaipur
Date: / /

Arvind Kumar Verma
M. Tech (DE)
ID: 2015PDE5090

ACKNOWLEDGEMENT

I express sincere thanks to my supervisor Dr. Amit Singh, Assistant Professor, Department of Mechanical Engineering, M.N.I.T., Jaipur, for providing me his invaluable guidance, support, supervision and useful suggestions. I am greatly honored for having had an opportunity to work with him. He constantly inspired and motivated me to achieve my academic goals. I am sincerely thankful to Dr. Dinesh Kumar, Dr. T.C. Gupta and Dr. Himanshu Choudhary who helped me beyond their duty at time of need.

Home is where one starts from; I express my deepest gratitude to my parents and my younger brothers for sharing their love and experience. The motivation I could not find within was rendered to me by them.

Place: Jaipur **Arvind Kumar Verma**

Date: / / **M. Tech (DE)**

ID: 2015PDE5090

Contents

Chapter 1 1

Introduction 1

1.1: Introduction 1

1.2: Reasons for dental implant failure 3

1.2.1: Failed Osseointegration 3

1.2.2: Peri-Implantitis (Infection) 3

1.2.3: Overloading 3

1.2.3: Foreign Body Rejection 3

1.2.4: Failure of the Implant Itself 3

1.3: Surface modification techniques 4

1.3.1: Overview of atomic layer deposition (ALD) technique 4

1.3.2: Overview of Thermal Oxidation (TO) 5

1.3.3: Overview of Electrochemical Anodization 5

Chapter 2 7

Literature Review 7

2: Literature review 7

Chapter 3 18

Failure Analysis of Ti6Al4V dental implant 18

3.1: Fracture surface cleaning 19

3.2: Fractography analysis 19

3.3: Conclusions 20

Chapter 4 21

Experimental Procedure 21

4.1: Material required 21

4.2: Sample Preparation 21

4.2.1: Mounting 21

4.2.2: Grinding 22

4.2.3: Paper Polishing 22

4.2.4: Cloth Polishing 22

4.2.5: Diamond Polishing 22

4.3: Preparation of Kroll's reagent 22

4.4: Preparation of tint etchant 23
4.5: RF magnetron sputtering coating 23
4.5: Operation procedure 26
4.6: Characterization techniques 30
4.6.1: Optical microscopy 30
4.6.2: Scanning Electron Microscopy 30
4.6.3: Atomic Force Microscopy 31
4.6.4: Micro-Hardness Study 31
Chapter 5 32
Result and discussions 32
5.1: Morphology Analysis 32
5.1.1: Optical micrographs 32
5.1.2: Scanning Electron Microscopy (SEM) 34
5.2 Atomic Force Microscopy (AFM) 36
5.3: Micro Hardness Study 41
Chapter 6 43
Conclusions and Future Scope 43
6.1 conclusions 43
6.2 Future Scope 43
References: 45

Tables

Table 1 30
Table 2 37
Table 3 38
Table 4 39
Table 5 40
Table 6 41

Figures

Figure 1: dental implant 1
Figure 2: SEM images of fractured dental implant in low and high magnification 20
Figure 3: Control unit of sputtering machine 24
Figure 4: sputtering device 25
Figure 5 : optical micrograph of Ti6Al4V surface etched with tint reagent 32
Figure 6: optical micrograph of Ti6Al4V surface etched with kroll's reagent. 33
Figure 7: optical micrograph of thin film of titanium oxide deposited by magnetron sputtering. 33
Figure 8: FE-SEM images of Ti6Al4V before thin film deposition. 35

Figure 9: FE-SEM images of titanium oxide thin film deposited by sputtering 35
Figure 10: AFM 2D topography of Ti6Al4V 36
Figure 11: AFM 3D topography of Ti6Al4V 37
Figure 12: AFM 2D Topography of titanium oxide thin film fabricated by reactive magnetron sputtering 38
Figure 13: AFM 3D Topography of titanium oxide thin film fabricated by reactive magnetron sputtering 39
Figure 14: average roughness 40
Figure 15: Root mean square roughness graph 41
Figure 16: Micro hardness graph 42

List of Abbreviations

TiO2	Titanium oxide
ALD	Atomic layer deposition
CVD	Chemical vapor deposition
PVD	Physical vapor deposition
FESEM	Field emission scanning electron microscopy
AFM	Atomic force microscopy
V	Vanadium
Al	Aluminum
Ti	Titanium
α	Alpha
β	Beta

Chapter 1

Introduction

1.1: Introduction

Implanting a biocompatible material at the area of damage to retain the normal functionality has been given special attention in the field of dentistry and orthopedics [1]. Today implants are used not only for diagnostic purposes but also for aesthetic needs [2, 3]. There are various kind of implants available today, such as cochlear implants, intacts, cardiovascular implants, prosthetic arthroplasty, dental implants, shoulder prosthesis, pacemakers, lumbar disc replacement, and acetabular implants [1].Different implant materials include polymers, composites, alloys, metals and ceramics depending on the area of their placement inside the body [1]. Specifically, for dental and hip applications, metals and alloys are areas of interest. Some of the required properties for metals and alloys to be considered for implants include corrosion resistance, wear resistance, mechanical resistance, low density, high biocompatibility, and absence of toxicity [4, 5]. Though the required implant properties are known, implant failure due to corrosion, wear, and lack of osseointegration is an on-going problem. Along with biological rejection, some of the potential non-biological reason for implant failure includes accidents and loosening of the implants due to regular physical or sport related activity [6]. Though metals and alloys possessing aforementioned properties do exist, failure of dental and hip implants still remains; moreover, three major causes of revision surgery over a long term are corrosion, wear and lack of osseointegration [1, 5]. This paper puts emphasis on materials used for implants, surface modifications, and novel techniques employed for modifying surfaces.

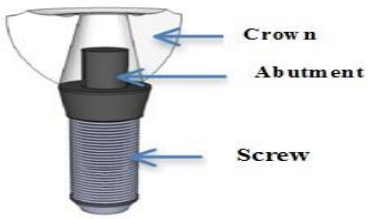

Figure 1: dental implant

There are three parts to the dental prosthesis: Screw, abutment, and the crown as shown in figure 1. The way these three parts play role in an implant is that the screw gets embedded into the gum, which serves as an anchor and comes in direct contact with the body tissues. Abutment supports the crown and it is also an interface between screw and crown [7]. Crown is the part that comes in contact with the oral cavity fluids and foods. Screw is the main area of interest in this study [8]. Moreover, because it comes in direct contact with the body tissues, immunological reaction and lack of osseointegration can be the major factor if the precautions are not taken with material selectivity. Failure of osseointegration may also leads to the micro-motions in the implants which can enhance the failure of implant. Therefore, in order for an improved lifespan of implants, better osseointegration is the key [9]. Screw portion of the implant is made up of Titanium grade 5 (Ti6Al4V alloy). This material is used due to its biocompatibility, high corrosion resistance, toxicity, and high mechanical resistance. However, since Ti6Al4V is not wear resistance, the debris released from the implant have potential to lead to some major problems such as toxicity, immunological rejection, revision surgery, and intervention in the other physiological activity depending on the site of the released wear debris. Therefore, action needs to be taken in order to prevent wear with the enhancement in osseointegration.

Pure titanium and titanium alloys are the mostly attractive materials for dental implant applications. Ti6Al4V is used as implant material in biomedical since a long period [10]. Titanium alloys which have high biocompatibility have been proposed and are currently under development [11]. There are two type of Ti alloys alpha and beta. β type alloys are composed of non- toxic elements such as copper ,nickel, iron, molybdenum, vanadium, zirconium ,tantalum etc. β type of alloys have BCC structure. α phase alloys contains neutral alloying element or α stabilizer such as tin ,aluminum or oxygen. α phase alloys have HCP structure. α phase alloys are stronger but less ductile than beta phase alloys because there are more no. of slip planes in BCC structured beta phase alloys than HCP structured alpha phased alloys. The β alloys have higher biocompatibility. These β alloys also have higher strength, hardness and toughness properties. Titanium alloys, especially Ti6Al4V are being used much more greater in medical and dental fields as implant materials because of it has superior biocompatibility, corrosion resistance property and specific strength compared to other metallic implant materials [12]. Alloy titanium is stronger than pure titanium. Al present in the TI6Al4V dental implant has many toxic effects such as encephalopathy, osteomalacia, increased risk of infection, anemia etc. To remove these toxic effects and increase the surface properties of Ti6Al4V, coating of TiO2 is generated. A nano structured coating of TiO2 is

fabricated by using conventional radio-frequency magnetron sputtering with Ti target.TiO_2 has three crystalline phases. They are anatase (tetragonal), rutile (tetragonal), and brookite (orthorhombic) [13]. The high affinity of Ti6Al4V for oxygen results in several oxides of differing crystalline structures

1.2: Reasons for dental implant failure

1.2.1: Failed Osseointegration

Osseointegration describes the formation of functional and structural connection between implant and bone. Some time it takes several months after the implant is placed. Often implant is failed because jawbone doesn't fuses properly with implant. Incorrect positioning, overloading, damage to surrounding tissues, insufficient bone density and overloading may be the cause for such type of failure.

1.2.2: Peri-Implantitis (Infection)

Bacteria may be present during oral surgery in lack of proper dental hygiene. This can cause peri-implantitis. Dental cement can also cause when it comes out during cementation and gets caught in the gums. It is one of the common complications that involve inflammation of gum or bone near the implant.

1.2.3: Overloading

It is a failure caused by undue pressure or force on crown or abutment. Overloading can disturb the osseointegration process. Overloading can cause fractured failure of implant. Patient those don't have sufficient mass on bone are not eligible to sudden loading.

1.2.3: Foreign Body Rejection

Patient's body may reject dental implant similar to organ transplants. In this case, patient's body sees implant as foreign object that doesn't belong to it and pushes it out.

1.2.4: Failure of the Implant Itself

This type of failure is attributed to bend or break of implant itself. Excessive and sudden loading can cause a crack or fracture in implant. Chemical re-sorption damages the surface of dental implant.

1.3: Surface modification techniques

In order to improve long term success of implants, various surface modifications are required that can increase corrosion and wear resistance, surface energy and thus surface wettability, improves and enhances osseointegration, while remaining atoxic. There are two methods through which the surface can be modified: chemical and physical. Chemical deposition technique involves chemical vapor deposition (CVD), sol-gel, and atomic layer deposition (ALD); moreover, physical deposition technique involves physical vapor deposition (PVD), evaporation, sputtering, pulsed laser deposition and molecular beam epitaxy (MBE). In this study, ALD have been employed to create TiO_2 layer on TiAl6V4.

1.3.1: Overview of atomic layer deposition (ALD) technique

ALD is used to modify the surface chemistry and to grow thin films with controlled mono-scale accuracy [14, 15]. It was developed around 1970s by Dr. Tuomo Suntola and his colleagues in Finland for electroluminescent displays [16], which was then extended in microelectronic industries and then in the research related to nano film deposition which progressed into semiconductor materials. In semiconductor, it was motivated to introduce the dielectric constant which improves the capacitance. One of the first ALD in the biological aspect was used to grow TiO_2 and Al_2O_3 on tobacco mosaic virus and ferritin. Generally, ALD is used to deposit any kind of surface coating on the implant surfaces using precursor, oxidant, and an inert gas to purge the non-reacted molecules from the chamber. This process contains four steps in one cycle to deposit one monolayer of a desired coating on the metal of interest. Growth rate of each cycle is calculated by the thickness of monolayer formed per cycle. Since the film is formed by precursor and linker, the thickness depends on the size of precursor and linker. And the duration of each cycle depends on the pulse duration set for precursor, oxidant, and purging. First step is to introduce a precursor which contains the molecule of interest along with varying number of protective organic group surrounding it. The basic requirements for precursors are they need to be volatile, thermally stable, and highly reactive [17]. Second step is to purge out the un-reacted precursor using an inert gas. Third step is to introduce a source that can act as a linker between two precursor molecules and it also rids of the organic molecules around the previous precursor. Fourth step is to purge the un-reacted linker source. This process is cyclic, and thus it allows to form the desired thickness on the metal substrate depending on the number of cycles been input for processing [13]. Some of the known advantages of ALD includes thin film deposition on the substrate with nano-scale accuracy and mono-layer thickness control [18]; low working

pressure and the self-limiting nature of ALD allows to maintain its conformality and uniformity throughout the large surface are of substrate .Thin film can be deposited at low working temperature which can be beneficial for polymer deposition, since some of the polymers decomposes at higher temperature; moreover, it produces the defect free film [19]. ALD allows formation of stoichiometric solid thin film with negligible impurities and retained surface roughness .Along with many advantages of ALD, there are some of the limitations which prevents its application such as cost and availability of precursor, low working temperature and pressure, and growth-rate [19].

1.3.2: Overview of Thermal Oxidation (TO)

Initially, thermal oxidation kinetics was studied on the silicon substrate by Deal Grove in 1965 due to the various silicon based device technology [20]. The main purpose of this technique during its earlier days included for the applications of silicon integrated circuits, MOS, capacitors, insulators, semiconductors, gas turbines, diesel engines, exhaust systems, biomedical applications and low cost solar cell material. The mechanism of oxidation depends on the diffusion of oxygen through the oxide layer to the initial layer of bulk where it reacts to form further substrate oxide .The steps for thermal oxidation, are

1- Transportation of the oxygen gas from its reservoir to the outer surface of the substrate.

2- Diffusion of the oxygen gas through the surface oxide layer towards bulk surface.

3- Reaction of the bulk surface with oxygen. Thus a thicker oxide layer is formed.

Some of the advantages of thermal oxidation include formation of oxide film with greater structural homogeneity, controlled film thickness, formation of high purity oxide film, conformal oxide growth, fairly simple process, and oxide is chemically bonded to the metal. Some of the disadvantages includes: Oxide may have defects, impurity redistribution and it consumes high amount of energy as it require high heat to facilitate diffusion of oxygen through the bulk metal.

1.3.3: Overview of Electrochemical Anodization

Initially, pure aluminum and silicon was anodized under acidic solution with constant applied voltage for various applications including electronics, optical and micromechanical devices. Anodization of aluminum and titanium for enhancing the corrosion resistance initially, pure aluminum and silicon was anodized under acidic solution with constant applied voltage for various applications including electronics, optical and micromechanical devices [21].

Anodization of aluminum and titanium for enhancing the corrosion resistance properties of implants by forming metal oxide layer was then developed in the later period .This technique produces nanotubular structures on the target material increasing the surface area of the treated sample; Moreover, due to this property of anodization, it has attracted scientists to utilize anodized samples for controlled catalysis, optical properties in photonic crystals, waveguides, 3D arranged Bragg-stack type reflectors, solar energy conversions or it can be used as a template for deposition of various coats for semiconductors, polymers, metals, or biomedical applications [22]. This process includes two basic phenomena for the formation of nanotubes .1) anodic oxidation where passive layer forms when anions specifically, O^{2-} or OH^{-1}, migrates and reacts to the metal surface which forms metal oxide and 2) chemical dissolution where self-organized degradation of the oxide layer takes place at the metal oxide and electrolyte interface due to the applied electric potential .In this process, initially, formation of the metal oxide predominates over chemical dissolution. Additionally, as the process continues, anodic reaction with subsequent chemical dissolution results into the enlarged pores forming nanotubes on the surface. The length and the diameter of the nanotubes can be controlled by applied potential, anodization time, and the pH of the electrolyte solution. Anodization can be performed with various combination of electrolyte solution 1) aqueous acidic solution with F^{-1}, 2) aqueous buffered solution, 3) non aqueous electrolyte containing F^{-1} ion with or without H_2O. Moreover, after the formation of nanotubes, anodized samples can be coated with various coats including HA which can enhance the cellular response property on the implanted metal. Some of the advantages of anodization includes its creation of nanotubes on the target surface, thus increasing the surface area for various applications, it is a controlled technique, forms uniform diameter nanotubes, simple technique, low working temperature compared to ALD, PVD or CVD techniques and cost-effective .

Chapter 2

Literature Review

2: Literature review

Ti has been used in the dental implant industry for the past 40 years since Dr. Branemark first introduced Ti dental implants. Ti implants can be divided into two groups commercially pure Ti and Ti alloys. Titanium alloys are mostly composed of Ti6Al4V. Ti widely used as the choice of biomaterial for dental implants because of its some important characteristics. Titanium is bio compatible, non toxic and non allergenic. Ti implants also have several drawbacks. The titanium particles can be released by fretting and wear debris from the implant surface. These particles could be spread into adjacent lymph nodes, which may cause immunologic reactions in living beings. However, there have been no cases of local or systemic reactions to titanium reported. Another important drawback of titanium is that the unwanted grayish color of the implant sometimes can show through thin gingival or mucosal tissue around the cervical area of the implant restoration. If gingival recession develops after implant placement or restoration, the unpleasant color of the titanium fixture will become visible. This potential drawback may jeopardize the esthetic outcome for implants placed in the esthetic zone and thus researchers have been searching for an alternative biomaterial with better esthetic outcomes. Recently, attention has been focused on zirconia (ZrO) ceramic as a suitable implant material due to its high modulus of elasticity, high mechanical strength, minimal reaction (biocompatibility) and better color mimicking of the natural tooth. In a finite element analysis, Kohal et .al [12] demonstrated that the magnitude and stress distribution were similar 6 between yttrium-partially stabilized zirconia implants and commercially pure titanium (cpTi) implants. Both cpTi and zirconia implants showed favorable and nondestructive stress distribution after loading. Comparing zirconia (ZrO) and cpTi threaded implants with machined smooth surfaces; found no statistically significant differences between the ZrO and cpTi implant groups in terms of bone to implant contact (BIC) and removal torque (RT). The amount of mineralized surface (MS; bone area/BA) at the four-most coronal threads showed statistically significant differences between the two groups and the ZrO implant group was preferred.

Guang-zhong Li, Quan-ming Zhao et al. [2016] [23] studied the coating of titanium oxide on Ti6Al7Nb. Ti6Al7Nb is used as an implant material because it has good corrosion resistance and high mechanical properties. But the presence of aluminum (Al) may cause to

ostemalacia, nervous system disorders and anemia. This limited its wide clinical use. In this study, a TiO2 nano porous layer was fabricated on a Ti6Al7Nb alloy. TiO2 film is fabricated by electrochemical anodic oxidation method. Scanning electron microscopy is used to determine the structure of TiO2 nano porous. Spectroscopy (XPS) was used to analyze the chemical compositions of the samples. Culturing rat osteoblast cells were used to evaluate the biocompatibility. This is found by results that TiO2 nanoporous layers comprise of mixed oxide containing TiO2 and a small amount of niobium oxides (Nb2O5) and almost no elemental aluminium. The inner layer forms disordered nanopores and outer layer of the TiO2 nanoporous layer comprises highly ordered nanotubes. The TiO2 nanoporous layer could support the adhesion, proliferation, differentiation and gene expression of osteoblast cells. Therefore, a TiO2 nanoporous layer could improve the biocompatibility of Ti6Al7Nb alloy.

A. Biswas, L. Li, T. K. Maity et al. [2007] [24] investigated the improvement of abrasion resistance of Ti6Al4V by nitriding and laser surface melting. Subsequently, they study the effects of laser surface treatment on corrosion resistance in simulated body fluids, and consider biocompatibility. A high-power continuous-wave diode laser using argon and nitrogen as shroud gas is used for laser surface treatment. The laser surface melting, the volume fraction of the β phase in the microstructure was lowered. Also, the volume fraction of the needle martensite was also increased. The formation of titanium nitride dendrite is formed by the laser surface nitriding. Improved micro hardness of up to 450 HV in the melting of the laser surface, in the case of laser surface nitriding, and improved to 900 to 950 HV compared to 260 HV of the as receiver substrate. Corrosion potential and primary potential for pit formation are increased by surface melting. However, when processed under the same conditions, the surface nitriding was shifted in a slightly more noble direction the corrosion potential, and increased the primary potential as compared with Ti6Al4V. The behavior of biocompatibility shows the viability of superior cells on surface nitriding and the survival rate of inferior cells on surface melting compared to the Ti6Al4V received as well.

Damian Wojcieszak, Michalmazur et al. [2015] [25] fabricated TiO2 thin coating by two types of sputtering methods- modulated plasma and with conventional. The films were fabricated on Si and SiO2 substrates. Coatings prepared by two methods were crystalline revealed by XRD. They found film fabricated by conventional method had anatase phase while fabricated by modulated plasma method had rutile phase. There was significant difference in the surface morphology as well as the microstructure at the thin film cross-

sections showed by investigations performed with help of scanning electron microscope. The mechanical properties of the obtained coatings were determined on the basis of nano indentation and abrasion resistance tests. The hardness was much higher for rutile structured films, while the scratch resistance was similar in both cases. Optical properties of both coatings were evaluated on the basis of transmittance measurements and were found that both films were well transparent in a visible wavelength range.

Xiaomian Wu, Xiaochen Liu et al. [2012] [26] N-TiO2/PEEK nano composites were made, for taking advantage of the properties of both PEEK polymer and n-TiO2. Bioactivity of these nano composites was assessed against a PEEK polymer control. The surface morphological effect or effect of roughness on the bioactivity of the n-TiO2/PEEK nano composites was also studied. In vitro studies, n-TiO2/PEEK was fabricated and cut into disks for physical and chemical characterization. And in vivo studies, n-TiO2/PEEK was prepared as cylindrical implants. Their presence on the surface and dispersion in the composites was observed and analyzed by SEM and XPS.

Francisco Lopez-Huerta, Blanca Cervantes et al. [2014] [27] examined the biocompatibility and surface properties of TiO2 thin films fabricated by DC magnetron sputtering. These films were prepared on a quartz substrate at room temperature, and annealed at different temperatures (100, 300, 500, 800, and 1100 C). For biocompatibility of TiO2 thin film, using the primary culture of DRG of Wistar rats, on the TiO2 thin film, was examined to incubate neurons on the control board between 18-24 hours. These neurons were activated by electric stimulation, and their ion current and action potential activity were recorded. The surface of the TiO2 thin film showed good quality, uniformity and roughness by XRD measurement. The Anatase -rutile phase Transition in the titanium oxide thin film of 500-1100 C taken place was shown in XRD measurement. The crystal grain size of this phase is 15 to 38 nm; it was possible to structure and crystal phase stability suitable for low temperature and high temperature of the TiO2 thin film. In the biocompatibility experiments of these films, Biocompatibility was shown to be good.

Vipin Chawla, R. Jayaganthan et al. [2008] [28] Thin film deposition parameters on the glass substrate by the magnetron sputtering method was significantly changed. Thin films were characterized by scanning electron microscopy, X-ray diffraction, and atomic force microscopy. The texture of the TI film, characterized by XRD, clarified the initial (1 0 0) preferred orientation. However, it is converted to (0 0 2) and (1 0 1) the direction to increase the substrate temperature and sputtering power. (0 0 2) and (1 0 1) orientation was found in

the film formed by sputtering having a pressure 5mtorr and 20 mTorr. This was observed an increase in the average surface roughness due to pressure from the atomic force Microscopy analysis, power, and temperature. Ti thin film deposited at a high substrate temperature showed a dense form by scanning electron microscopy. The crystal grain size of the TI thin film shows an increasing tendency of the evaporation parameters to be changed by X-ray diffraction.

S.L Sing et al. [2016] [29] The effect of process parameters and design on dimensional accuracy and compressive behavior of cell lattice structures prepared using selective laser fusion (SLM) was investigated. Two unit cell types, truncated cubes and square pyramids & octahedral from Computer support systems for organizational scaffolding, used an in-house developed library system. The powder adhesion occurs on the strut of the lattice structure. Elastic constants in lattice structure compression increased with relative density increase, ranging from 7.93 ± 2.73 MPa to 7.36 ± 0.26 GPa. Distributed analysis is also done to examine the importance of different design parameters and processes for the compressive strength and dimensional accuracy of lattice structures. Processing parameters, such as laser scanning speed and laser power, do not affect the elastic constants any more, but have a significant effect on the adhesion of struts, which affects the dimensional accuracy. However, geometric design parameters, such as strut diameter and unit cell type, have a significant effect on elastic constants, but there is no dimensional accuracy of the lattice structure. The thickness of the strut's powder adhesion decreases with the increase in laser power and laser scanning speed.

Peter J. Kelly, Justyna Kulczyk-Malecka et al. [2003] [30] Titanium dioxide thin films are durable, chemically stable and have high refractive index and good electro/photochemistry courtesy. Widely used as an anti-reflective layer for optical devices, large area glazing products, microelectronics devices, and self-cleaning surfaces. Coating may have an amorphous or crystalline structure that can get three crystalline phases of titanium oxide: anatase, rutile and brookite, although the latter is seldom found. However, the structure of the TIO2 film is sensitive to the deposition conditions; it is known that it can be modified by heat treatment after deposition. In this study, by the reactive sputtering method from the metal target, the titania coating was deposited on the soda lime glass substrate. The magnetron was driven in the mid-frequency pulse DC mode. The evaporated film was analyzed by microscopic Raman spectroscopy, X-ray diffraction (XRD), Atomic force microscopy (AFM), and scanning electron microscopy (SEM). The selected coating was annealed and re-

analyzed at temperatures ranging from 200 to 700 C. In this way, although there was weak evidence of Nano crystallinity in the deposited film, these were observed that the amorphous low temperature structure is mainly converted into a strong crystal structure at 400 C or more annealing temperature.

Ab. Benyoucef, Am. Benyoucef et al. [2007] [31] This last decade, TiO2-based solar cells are one of the most concentrated studies, because they present a very low coastal production perspective and offer attractive features that facilitate market entry. Especially after Gratzel's work, it is stated that it is possible to have an excellent efficiency of 11% on very low coasts compared with silicon solar cells. Sol-Gel is the most utilized method for coating a low-coast TiO2 film on any substrate. The main problem of this method is however related to the bad electrical connectivity of the TiO2-Nanoparticules between them with the substrate, which is the result of the chaotic nature of the film. To solve this problem, the magnetron is used to coat the nano crystalline TiO2 thin film on a non-heated substrate (conductive glass or polymer). In this work, we focus on the effect of the coating parameters on the microstructure of the rejection film. For this, authors deposited a different TiO2 thin film argon and oxygen gas flow ratio. X-ray diffraction (XRD) measurements are affected by samples that know the phase (anatase or rutile). This form was revealed by a scanning electron microscope (SEM) and atomic Force microscope (AFM). The coarse average square root (RMS) was inferred from the AFM data. Incidentally, the results of XRD, the rutile phase is shown to be dominant in the low-pressure region (0.3 - 0.6 Pa) but anatase phase is more in high pressure range. At constant value of the pressure when the flow ratio O2/Ar changes the crystal orientation of the anatase phase is slightly modified. Therefore, the optimal solar power parameters were estimated from the characteristics of morphology and structure.

Ji Chon Lim and Kyu Jeong Song [2014] [32] The conventional RF magnetron sputtering method is used to film TiO2 thin films on Si substrates using metal Ti or TiO2 targets. Then, the evaporation parameters (substrate temperature(TS) , RF sputtering power, the gas flow ratio of O2/ (Ar + O2), and the effect of deposition time) was investigated in the phase of the film using X-ray diffraction (XRD) and a scanning electron microscope (SEM), to obtain each information on the surface image/film thickness of the film phase and film. TiO2 film deposited at TS higher than 300C using a metal Ti target, showed the dominant presence of the rutile phase. For membranes grown with a TS 300C at different gas flow ratios of O2/ (Ar+O2), the amount of the rutile phase decreased gradually as the flow of oxygen gas decreased. However, the anatase phase was formed when the O2/ (Ar+O2) flow was 0.2. On

the other hand, when the film is fabricated at 0.1 flows of O2/ (Ar+O2) using a TiO2 target of temperature 50 C- 200C, both the phase of anatase and rutile gradually decreased as TS grew. For TiO2 film fabricated at a variety of gas flow ratio of 0- 0.4, O2/ (Ar+O2) at a constant TS 200C using a TiO2 target, although the anatase phase gradually decreased, the rutile phase was gradually increased as the gas flow ratio increases.

L. Le Guehennec, A. Soueidan et.al [2007] [33] The composition and surface roughness of titanium dental implants were thought to be related to the osseointegration rate. Both bone fixation and biomechanical stability are supported by coarse-surface implants. The same coordinates as bone healing facilitated by the conductive phosphoric acid coating, leads to rapid biological fixation of the implant. Another method is used to apply conductive coatings to increased surface roughness and titanium dental implants. Acid etching, polishing blasting, calcium phosphate coating, anode, surface treatment such as its properties and corresponding surface morphology is described. The exact role of topography and surface studies in the early events of the dental breast augmentation osseointegrasion remains less understood. The future purpose of dental implants should be to develop the surface with control and standardized topography and chemistry. This approach is the only way to understand the interaction between the surface of cells, tissues, proteins and implants. The local release of bone irritation or absorbent around the implant is also the quality and quantity of the bones may be bad and difficult to deal with the clinical situation. These therapeutic strategies should eventually strengthen the osseointegration process of dental implants for their immediate loading and long-term success.

Zhou Linxi, Yang Quanzhan et al. [2014] [34] Biomedical materials used in orthopedic and dental implants have with good corrosion resistance and mechanical properties. But there may be a stress shield due to the significant difference in the elastic modulus of the implant and the human bone. The elastic modulus of the porous metal is lower than the dense metal. Therefore, the pore parameters can be adjusted to make the elastic modulus of the porous metal equivalent to that of the bone tissue. The structural conditions for developing bones can be provided by an open porous metal with pores connected to each other. This may help to enhance the biological combination of implants and bone tissues. As a result, porous metal implants and related research technologies have been attracting more and more attention due to the excellent features of this material. In the research field of additives manufacturing, selective laser melting (SLM) and electron beam melting technology (EBM) are important. They have the advantage of forming metal parts of any complex shape that is suitable for the

preparation of porous metal implants with direct complex shapes and fine structures. The SLM and EBM of porous metal implants are a new manufacturing technology. The current state of SLM and EBM technology and the progress of research on porous metal implant formulations using SLM and EBM are designed to understand the requirements of individual design and manufacturing, and the biological suitability of materials. We consider the direction of future research and the existing problem of the porous metal implant by SLM and EBM.

A. Pazo, E. Saiz et al. [1998] [35] Ti-based implants coated with bioactive substances can form hydroxyapatite layers in Viva. These coatings are easily bonded between prosthetics and bones. It also improves the long-term stability of the implant. The authors describe a new pathway for coating the Ti alloy using an active silica-based glass. The new family of bioactive glass is developed having good physical suitability with Ti. The glass powder is painted on a metal substrate to fabricate a dense coating and the assembly is fired to make the glass flow, adhering to the metal. X-ray diffraction and electron microprobe used to study the reaction that occurs between glass and metal in this process. By controlling the firing conditions (atmosphere, temperature and time), it was prepared by tailoring a good uniform coating of adhesion to the metal to the glass composition. The physical characteristics of eyeglasses and their behavior in simulated body fluids are also reported.

Kathyayini et al. [2013] [36] The reactive DC magnetron sputtering method enables titanium oxide (TiO2) films to be fabricated on titanium (Ti) substrates that are completely washed at different evaporation temperatures. The field-radiated scanning electron microscope (SEM) and X-ray diffraction (XRD) are used for microstructure and morphological properties of TiO2 thin films, and it is revealed that the sputtered film is present in the oblique phase. As calculated from XRD, the crystallite size of the film was changed between 19-25 nm. Contact angle measurement was used to analyze the hydrophobic/hydrophilic of the TiO2 film. Surface Modification Ti substrate surface has an activity shown by the formation of apatite of the deposited film after immersion in simulated body fluids. Kinetic clotting time method was used to evaluate the blood suitability in the body of both the surface modification and the unmodified substrate.

Danuta Kaczmarek, Jaroslaw Domaradzki et al. [2012] [37] Studied on the hardness of nano crystalline TiO2 thin films was prepared using low-pressure hot target reactive sputtering (LPHTRS) and high energy reactive magnetron (HERMS). The metal Ti target was sputtered under low pressure of oxygen-operated gases in both processes. After obtaining

a thin film of anatase structure after deposition by LPHTRS, it was recrystallized to the rutile structure after the post annealing at 1070 K. For Annie there is an increase in the average crystallite size from 33 nm (anatase type) to 74 nm (for rutile). The HERMS process is a change in the LPHTRS process, which supplies power to the magnetron and increases the amplitude of the unipolar voltage pulse. This will eventually increase the total energy of the deposited particles on the substrate, which caused a dense, nano crystalline (size 8.7 nm crystals) TiO2 thin film with a rutile structure that is formed directly. With the indentation the hardness of the film was determined. As a result, the thin film produced by HERMS, Nano crystalline TiO2-rutile has a high hardness (14.3 GPa), TIO2-anatase film produced in LPHTRS showed a low hardness (3.5 GPa). LPHTRS membranes were re-crystallized with an additional annealing. The change in the thin film structure from anatase to rutile resulted in a rise in the hardness of the film. Therefore, the herms process can produce a TiO2 rutile structure directly, and has twice the hardness than the film of the rutile produced by LPHTRS.

Claudia Fleck, Dietmar Eifler [2010] [38] Implants have become more important in all areas of medical science. Orthopedic and dental implants are applied routinely to wear with high mechanical loads and multi-axes, step fatigue such as friction. One major challenge of these implants is to maintain these loads which are highly corrosive and are complicated by the need to survive in the body's electrolytes (proteins, enzymes, salts). Titanium and its alloys, compared to other metal implant materials, do not perform surface reactions, even though they have given exceptional biocompatibility for the formation of highly stable oxide layers in a physiological environment. Such reactions, for example, adsorption of ion exchange and protein, determines the stability of the bone implant interface, as a result, mechanical activation of the surface plays an important role. The authors ' works show the current knowledge of the corrosion, fatigue, and corrosion fatigue behavior of titanium and its alloys, and are particularly focused on the effects of simulated conditions in vivo.

M.A.L. Hernandez-Rodriguez, G.R. Contreras-Hernandez et al. [2014] [39] after six months of service, A Ti6Al4V Dental implants failed to ruin. This kind of failure is rare in the short term like six months. However, in this case, the fracture was shown in the inner screw used for fixing the abutment. Visual inspection, chemical analysis, metal, micro hardness Test, and EDS (Energy dispersive X-ray spectroscopy) was subjected to macroscopic and microscopic fractography observation using a scanning electron microscope. In addition, finite element analysis (FEA) was carried out to clarify the stress

scenario of the failure. The test results, the failure are facilitated by the bone re-sorption, leading the state of the cantilever, resulting in an overload system with a cyclic high level of stress. This state, together with the concentration coefficient due to the rough surface finish and geometric changes seen in the screw, was caused a crack propagated to the failure of the component.

Ken'ichi Yokoyamaa, Tetsuo Ichikawab et al. [2001] [40] Ti and its alloys are becoming more and more focused on their use as biomaterials. But the delayed fracture of the titanium dental implant has been reported, and the factors that affect the corrosion and acceleration of fatigue must be determined. The authors analyzed the fracture surface of the acquired titanium screw and the metallurgical structure of the dental implant system. They found that the shear cracks on the outer surface started at the thread root and propagated to the inner section of the screw. The resulting screw was to absorb a higher amount of hydrogen than the as received sample revealed by gas chromatography. The crystal grain structure of the titanium screw immersed in a solution known to induce hydrogen absorption showed the same characteristics as the obtained screw. The authors concluded that titanium in the biological environment could absorb hydrogen and cause delayed fracture of titanium implants.

M. Gahlert, D. Burtscher, I. Grunert et al. [2011] [41] The purpose of the authors' research was macroscopic and microscopic failure analyses of fractured dental implants of zirconia. Out of 170 inserted implants, 13 fractured one piece implant in situ period of 36.75 ± 5.34 months from the range of the period to 20 to 56 months, the median 38 months were prepared for macroscopic and microscopic failure analyses. These 170 implants were inserted in 79 patients. The medical history of the patient was compared with the incidence of fractures in order to determine the cause of the implant failure. The implant had a diameter of 3.25 mm, and 12 fractured implants with a diameter of 4mm. The fractured implant is located on the anterior side of the maxillary and mandible; patients with a 4 mm diameter implant fracture were adversely affected by strong grinding. With scanning electron microscopy it can prove that in all cases, mechanical overload has caused the destruction of implants. You can exclude ceramic material and uneven internal defects. However, the scratches caused by a notch and surface sandblasting led to localized stress concentrations that led to the aforementioned mechanical overload by bending load. In this study, we have identified a close to 10% rupture rate in the follow-up period of 36.75 months after the artificial load. 92% of the fractured implant reduced the so-called diameter implant (3.25 mm diameter).

Improvements in ceramic materials and changes in the shape of the implant should reduce the failure rate of small ceramic implants. Nevertheless, due to the lack of proper laboratory testing, only clinical trials have been proven to reveal how much failure rates can be reduced.

Keren Shemtov-Yona, Daniel Rittel et al. [2012] [42] The purpose of authors' study was to analyze the external failure mode and to be able to evaluate the relationship between the fracture mode and fatigue behavior of the implant. After being tested for fatigue performance for this, 80 fractured dental implants were analyzed. A macroscopic failure analysis was performed to evaluate the resulting fracture mode. Scanning electron microscope (SEM) and fractographic analysis was carried out. The four characteristic fracture trajectories were identified, and Macro fracture mode analysis was performed. All 5 mm implants were fractured by the neck and the screws on the base. In a group of 3.75 mm, 44.4% fractured at 55.5% in the second thread of implant neck and implant. 52% of the 3.3 mm fractured implant had it in the implant second tread and 48% of the implant's third thread. In the metal part of the implant, another breaking trajectory was revealed that a thin metal cross section and a sharp notch coexist. By analyzing the sequence of secondary parallel cracks, the fault minute and fatigue properties as fractures at a relatively low magnification, a classic fatigue streak of high magnification by scanning electron microscopy is obtained. The result of this study is that the long-term fatigue performance of the implant is ensured and the appropriate implant design is important.

Mohamed A. Hussein, Abdul Samad Mohammed et al. [2015] [43] In the field of biomedical medicine, metals are widely used for a variety of applications such as joint replacement, orthopedic fixation, internal support and biological tissue substitution such as tooth roots and stents. Stainless steel, CO alloys, and Ti alloys are metals and alloys primarily used in biomedical applications. Wear and abrasion resistance determine the service period of the metal biomaterials. Implants loosen for abrasion resistance due to the release of incompatible metal ions in the body. In addition, several reactions due to adhesion of tissue wear debris may occur. Therefore, it is important to develop a high-abrasion bio-material for longevity of the biomaterials. The purpose of the work of the author is to check the current state of knowledge of the wear of metallic materials, and how the manufacturing process developed in terms of the type of alloy the wear was affected by the properties and conditions of the material.

Oguz Kayabasi, Emir Yuzbasioglu, Fehmi Erzincanli [2006] [44] In the long-term success of dental implants, reliability and implant bone interface and implant stability-the

abutment plays a major role. The success of treatment relies on many factors that affect the bone – implant, implant – abutment and abutment – prosthesis interface. The effects of dynamic load and fatigue were investigated by the author. In this study, we investigated the static dynamic fatigue behavior of implants. 5-minute dynamic load fatigue life implants applied to occlusal surfaces are computed based on Soderberg, Gerber, and Goodman and average stress fatigue.

A. Sliwa, L. A. Dobrzański, W. Kwaśny, M. Staszuk [2010] [45] Worked to determine the micro hardness of film and stress obtained in the PVD process. For this purpose they used a finite element method. The results obtained by the experiment were analyzed. They simulated the micro hardness and stress of the TiN and TiC coats obtained on the high speed steel ASP 30 by magnetron PVD process. The basis of the tension obtained as a result of the depression of the surveyed surface indenter authors get a map of stress, deformation, coat analysis, and they calculated micro hardness. Based on the tension of the research task obtained by computer simulation in the ANSYS software environment, it is possible to calculate the micro hardness of the coating; the results were compared with the micro-hardness data of the coat received by the physical examination using the Vickers method. From the results of the simulation based on the finite element method, it is possible to calculate the mechanical properties of the film obtained by PVD treatment.

Zhaohui Shan, Suresh K. Sitaraman [2003] [46] It is an issue to experimentally determine the elastic and plastic properties of thin films below the thickness of 1 mm. The authors presented a methodology combining finite element modeling and nano-indentation technology characterizes the mechanical properties of titanium thin films. The elastic properties of titanium thin film (Young's modulus) does not change compared to the bulk titanium. In addition, the plastic properties of the titanium thin film (yield stress and strain hardening index) were shown to be higher than those of bulk titanium. The methodology described in this article can be used to study the mechanical properties of other thin films or small amounts of materials. . The objectives of this research are-

1: Failure analysis of Ti6Al4V dental implant.

2: Removing the defects of Ti6Al4V by thin film deposition of TiO2.

3: Study the properties of Ti6Al4V dental implant and thin film by using different characterization techniques.

Chapter 3

Failure Analysis of Ti6Al4V dental implant

The use of dental implants as a treatment option for the rehabilitation of deficient teeth is met with a very high success rate. Despite this, the complications associated with this treatment the presence that could eventually lead to loss of both implants and prosthesis. The failure of the slow treatment can be caused by a mechanical complication that may include screw loosening and/or cracks, a crack in the abutment and implant. Systematic review, about the survival and complications of dental implants, after a follow-up time of at least five years, showed that mechanical complications are common, including the incidence of 2.5% abutment and screw fractures, followed by a 10-year follow-up time. The fracture of the implant showed a relatively rare event, a cumulative incidence of 1.8 percent after a follow-up time of 10 years. A long-term retrospective cohort study that evaluates the results of implant therapy over 10-16 years mechanical, complications such as the fracture of the implant, the fracture of the abutment, the screw of the implant, and the fracture of the prosthesis porcelain showed all incidence of 31% compared to 16.9% of biological complications. Today, dental implants are made with either pure (CP) titanium or titanium alloys. Among the latter, Ti6Al4V was the main biomedical titanium alloy used in the manufacture of dental implants. The high physical mechanical properties of these materials in other words, relatively low young modulus, high fatigue and corrosion resistance, excellent biocompatibility, they are all important properties of titanium alloys suitable for implant materials. Detailed fracture analysis of removed broken dental implants is very rare in dentistry and biomechanical literature as well. This is because the incidence of fractures in dental implants and implant parts is quite low. Most fractured implants due to the difficulty of getting them remains in the alveolar bone after fracture. In most cases, the fracture of the implant, which is essential to the fracture analysis, is destroyed or is greatly damaged by making the fracture analysis impossible. In parallel, there is no clear and decisive technical directive for the handling and preservation of broken implants and implant parts.

3.1: Fracture surface cleaning

Fractured part of dental implant is cleaned to remove blood/ soft tissues, organic and inorganic materials stick to it. To remove blood / soft tissues we put the fractured implant in the 100 ml beaker and fill it with sodium hypochlorite 3% solution for 10 minutes. For removing organic layers we put the fractured implant in the 100 ml beaker and fill it with acetone for 30 minutes. For removing inorganic layer similar process is done with EDTA 17% for 20 minutes.

3.2: Fractography analysis

The fractographic analysis of fractured Ti6Al4V dental implant is carried out by scanning electron microscope. The appearance of screw fracture surface at low magnification can be assessed. The fracture surface is matte, without cleavage signs. It points to ductile failure after previous plastic deformation. Detail of fracture surface confirms the above mentioned character of failure. According to its morphology, it can be specified as the transcrystalline ductile failure with dimple morphology. After SEM analysis of the fracture surface a longitudinal section was prepared from fractured screw. Detail of its microstructure close to the fracture is shown. The microstructure observed by optical microscope is polyedric, fine grained, uniform. It is heterogeneous, composed of α and β phases. Changes that could be related to the fracture of screw were revealed by the SEM observation of the same longitudinal section. There are numerous cavities clearly visible near the fracture. These cavities may result from the local overheating and melting down of material. Ti6Al4V has a very low thermal conductivity, which could occur after a blunting of the tool used during a cutting process .Ti6Al4V has a relatively high coefficient of friction. The above mentioned character of the fracture seems to correlate with this explanation.

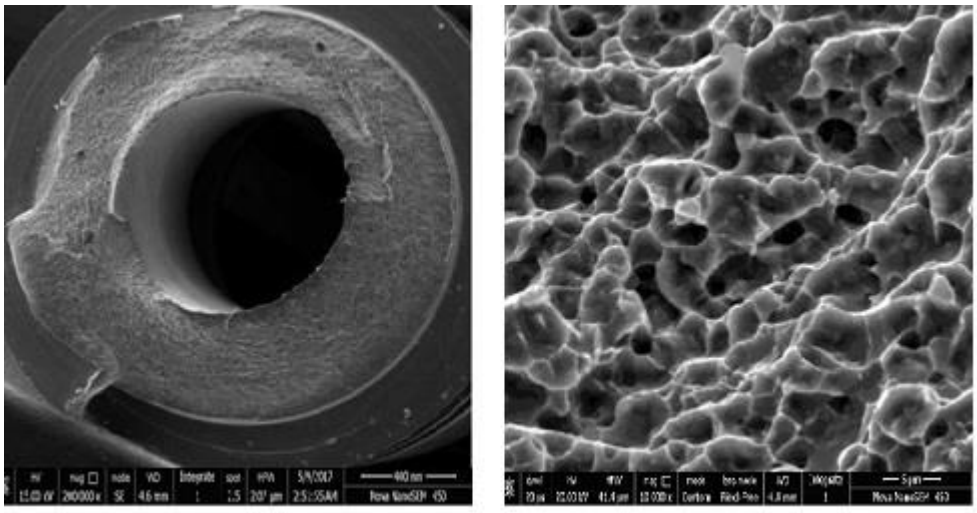

Figure 2: SEM images of fractured dental implant in low and high magnification

Ti6Al4V alloy is often used in dental implantology. It has high strength properties but its disadvantage is poor tribological properties such as wear and friction.

3.3: Conclusions

Fractographic analysis of fracture surfaces of the broken implant revealed that it is the transcrystalline ductile failure with dimple morphology.SEM display of longitudinal section reveals changes in the microstructure, which may be related to the fracture. Clearly visible cavities near the fracture surface may result from the local overheating and melting down of material which could be related to a blunting of the tool used during a cutting process. In conclusion it can be said that observed fracture of dental implant was not caused by a low quality of material but by a mistake during a cutting process. Some marks are seen at outer surface of implant these may be due to surface wear, may lead to a fracture failure. There is enough wear on outer surface of fracture. This may be the reason of crack initiation in implant.

Chapter 4

Experimental Procedure

In this chapter, we fabricate a thin film on Ti6Al4V dental implant for removing the scratches of machining process and increasing the surface hardness so that wear resistance may increase.

4.1: Material required

We required one pieces of fractured Ti6Al4V dental implant for study and film deposition on them. Epoxy resin, hack saw, wiring pipe and hardener for mounting of dental implant for the ease of grinding and polishing processes. Emery papers of sizes grades 150, 200, 300, 600, 1200, 1500 for grinding process. Hydrofluoric acid and nitric acid are used to prepare kroll's reagent. Oxalic acid is used to prepare tint reagent. Both kroll's reagent and tint reagent are prepared in de ionized water. Diamond and alumina slurry are used for polishing purpose. Ti target material and oxygen are used in coating of thin film of TiO2 on Ti6Al4V dental implant. Acetone is used for cleaning purposes.

4.2: Sample Preparation

4.2.1: Mounting

The sample should also be degreased and dried before mounting to ensure adequate adhesion of the mounting media. Careful consideration is also necessary for making proper metallurgical mount. The first consideration is choosing the most appropriate mounting medium. Ti6Al4V is a very abrasion-resistant material, and it is essential that the titanium alloy be mounted correctly to produce a quality metallographic sample. The selection of mounting material has a significant impact on edge retention and the surface flatness of the mount. Failure to use the proper mounting media may cause rounding of the interface between the mount and sample, resulting in poor edge retention. It can also cause rounding or faceting of the overall mount surface. There is a probability of heat treatment in hot mounting process so we used cold mounting process so that micro structure and phase of Ti alloy would not change. For cold mounting of dental implant we used epoxy resin and hardener. First we cut a wiring pipe of length having that of dental implant by hack saw. Then stand dental implant within this. These whole things are put above a glass slide. After mixing epoxy resin with hardener in 10:1, is poured within wiring pipe incorporated dental implant. After 10 hours dental implant is completely mounted in wiring pipe by resin.

4.2.2: Grinding

Grinding of crude and rough samples was done on a belt grinder. Grinding was done to produce smooth edges .The purpose of grinding is to remove the damage caused by the sectioning process. Sectioning methods, such as slow-speed wafering, that do not introduce much damage into the sample do not require extensive grinding and decrease sample preparation time.

4.2.3: Paper Polishing

Paper polishing was done on seven types of emery papers graded as 150, 200, 300, 600, 1200 and 1500. These papers have abrasive particles fixed on their surface. 150 grade emery paper has more roughness than the others. The grit size of the paper decreases from 150 to 1500. We rubbed sample on emery papers with increasing in grade numbers, starting with 150 grade onward. Paper polishing can be done by manual or automation. Paper polishing was done to remove roughness of the material.

4.2.4: Cloth Polishing

After paper polishing, the next step was Cloth polishing. Cloth polishing was carried out on a velvet pad on a cloth polishing wheel. This was used as a pre-requisite for finishing of the polishing process. Alumina is poured on rotating cloth wheel and sample is pressed gently against the wheel. Cloth polishing is carried out to remove the scratches in sample.

4.2.5: Diamond Polishing

After cloth polishing diamond polishing is carried out. It is last step in process of removing scratches. Diamond suspension with fluid is poured on the wet cloth attached to rotating wheel and sample is pressed against the rotating wheel and scratches are removed. There are different grade of diamond suspension. Starting from high grade to lower grade diamond suspension is used.

4.3: Preparation of Kroll's reagent

First etchant used for optical microscopy is Kroll's reagent. Reagent is prepared according to empirical formula. To prepare this we used 2 ml of hydro fluoric acid, 10 ml of nitric acid and 88 ml of deionised water. First we were taken 88 ml deionised water in a flask then added 10 ml of nitric acid in it and then added 2 ml hydro fluoric acid in it. The solution was stored for the further use.

4.4: Preparation of tint etchant

Second etchant used for optical microscopy is tint reagent. Reagent is prepared according to empirical formula. To prepare this we used 20ml of hydro fluoric acid, 20 gm of oxalic acid and 98 ml of deionised water. First we were taken 98 ml deionised water in a flask then added 20 gm of oxalic acid slowly in it and then added 2 ml hydro fluoric acid in it. The solution was stored for the further use.

4.5: RF magnetron sputtering coating

It is an ALD process of thin film deposition. In this technique gas ions are created in very hot plasma. These accelerated gas ions hit on target material at very high speed. These impacting ions remove material from target material which in turn hit the substrate and stick to it. Typically very low gas pressure is maintained in chamber in range of 3to 50 mtorr for sustaining the plasma. There are always some positively charged gas ions available to ignite the plasma due to natural cosmic radiation. A negative potential is applied on target in DC-sputtering .this accelerate positive ions which in turn hit target with increased velocity. It is up to several hundred volts which accelerate the positively charged ions to the target. These accelerated ions further create energetic electrons which are called secondary electrons. These secondary electrons also hit the target and remove material. A magnetic ring is use to increase the ionization of electrons. It is put below the target. This ring traps secondary electron and circulates to the target. This process is called as magnetron sputtering. DC-sputtering can be use for conducting materials only like metals and doped semiconductors. Bombardment of positive ion, charge the surface of target material. This leads to dyeing of ionic current. For removing this problem, radio frequency AC voltage is applied. It let not build up the charge on target material as in case of DC sputtering. This process is called as RF-magnetron sputtering. Argon is used in sputtering for plasma creation. Nitrogen and Oxygen are also used in reactive ion sputtering. Oxygen and nitrogen are reactive gas, chemically combine with the target material and forms another material. The substrate holder can be heated up to 850 C for further enhancing reaction rates. It can change the morphology of the deposited films. RF-power can be applied on the substrate holder to sputter clean samples before deposition by the machine. Film uniformity can be improved by rotating the substrate during the process of sputtering. Rotation of substrate is necessary for heated deposition and may also be applied on room temperature depositions.

Figure 3: Control unit of sputtering machine

Figure 4: sputtering device

4.5: Operation procedure

Following steps are followed in coatings of TiO2 and Ti on Ti6Al4V dental implant.

4.5.1: Mount Sample

Wear clean gloves so that contamination of chamber can be eliminated. There is a round on sample holder which sample is to be mounted. On this sample holder sample can be mounted by using washers and screws. But in our case, as our sample is very small, we used a tape to stick sample on holder. This tape is able to sustain temperature up to 400C .we ensured that sample is stuck properly by shaking holder.

4.5.2: Vent Load-Lock Chamber

The load lock turbo pump power switch is turned off which labeled as Load-Lock Vacuum Pumps for venting the load –lock chamber. Due to this the turbo and mechanical pumps are shut off and the turbo pump's delayed vent valve activated.

4.5.3: Open Load-Lock Chamber

When pressure of the load-lock chamber is reached to atmospheric pressure, aluminum load-lock cover is lifted. It is placed on the four rubber pads on the top of table. Face of it should be down.

4.5.4: Load Sample

We positioned the substrate holder on the transfer arm. It is important that orientation of sample holder should be correctly so that there might be maximum deposition of target material on substrate.

4.5.5: Replace Cover

Place the aluminum load-lock cover uniformly on the load-lock transfer port.

4.5.6: Pump Chamber

Turn on power switch of Load-Lock Vacuum-Pump to pump down the load-lock chamber. It will take about 5-10 minutes for pump-down process. it will save the sample transfer to the main chamber when pressure of load lock chamber is below 1*E-5 mbar.

4.5.7: Open Gate Valve

The transfer gate valve could be opened safely the pressure of load-lock chamber is below 1*E-5 mbar. The gate transfer valve could be opened by turning the transfer valve crank in counter-clockwise until it stops.

4.5.8: Position Transfer Arm

Looking through the viewport, the substrate holder height could be raised by using joystick to allow enough clearance for insertion of the transfer arm. Gently push the transfer arm from right arm to the left until it hits its mechanical stop.

4.5.9: Engage Substrate Holder

By moving the joystick left or right, the propeller blades are rotated to align with the recessed blade .these recessed blades are mounted on the sample holder. The propeller blades are lowered into the recess on top of the substrate holder by moving the joystick. The blades are lowered into the substrate holder until a slight bend in the transfer arm is detected. Next, the propeller blades are rotated 30^0clockwise to engage the sample holder mount manually.

4.5.10: Extract Substrate Holder

Substrate holder is lifted from the transfer arm by moving the joystick up. The substrate holder rose to the desired process distance. The default process distance was indicated by the alignment mark on the steel ruler mounted next to the bellows.

4.5.11: Retract the Transfer Arm

Transfer arm is moved slowly out of the main chamber until it come to rest against the mechanical stop.

4.5.12: Close Gate Valve

Handle is turned clockwise to close the transfer gate valve. An audible click could be heard just before the gate valve was completely closed.

4.5.13: Sputter Deposition

In sputter deposition following step takes place.

4.5.13.1: Start Sample Rotation

The speed adjust knob on the rotation controller is turned on slowly to the desired level for beginning substrate rotation .We visually checked that if the sample rotation was smooth and level. If this is not the case, the propeller blades may not be adequately locked into the sample holder. A rotation setting of 50% is good for most runs. Higher rotation rates should be used for short duration runs for improving the uniformity.

4.5.13.2: Activate Substrate Heater

The rotary heat switch and heater controller switch is turned on in order to operate heater. Substrate holder must be rotated for uniformly heating of substrate. Heater can be operated manually. But heater operation by computer controller is better. The SHQ-1SR substrate heater controller can heat the Inconel sample holder up to a temperature of 850C.

4.5.13.3: Start the Deposition Process

Process control computer is used to create and run process. Processes can also be run manually. For this, the VAT controller should be in Remote mode. For starting the process, clicked on the **Run** Process button and Opened the desired process recipe. A dialog box would appear with a short checklist. All checklist items were satisfied, so clicked on the **OK** button, which would started the process. If checklist items were not satisfied then clicked on **Cancel** .At the end of the process, a dialog box would appeared indicated that the process had been completed.

4.5.14: Sample Unloading

Steps for sample unloading are given below.

4.5.14.1: Turn Heater off

Substrate heater is turned off by turning the Heat switch on the heater controller counter-clockwise to the off position.

4.5.14.2: Stop Sample Rotation

Sample rotation is stopped by turning sample rotation knob in counter-clockwise to stop sample rotation. Sample holder is rotated back to the position it had been when positioned on the transfer arm by using the left-right joystick controller.

4.5.14.3: Open Gate Valve

Chamber pressure in the load-lock should be below 1.0E-5 mbar for opening the gate valve. Gate transfer valve is opened by turning the valve crank counter-clockwise.

4.5.14.4: Position Transfer Arm

Joystick is used to raise the substrate holder to allow enough clearance for insertion of the transfer arm. The transfer arm is pushed to the left until it hit its mechanical stop.

4.5.14.5: Disengage Substrate Holder

The sample holder is lowered onto the transfer arm by a joystick. Substrate holder is lowered until a slight bend in the transfer arm was detected. Now, the propeller blades are lowered 30^0 counter-clockwise to disengage the propeller blades from the sample holder mount manually.

4.5.14.6: Retract the Transfer Arm

The transfer arm is moved slowly out of the main chamber until it came to rest against the mechanical stop.

4.5.14.7: Close Gate Valve

Manual transfer gate valve is closed by turning the handle clockwise. Just before the gate valve was completely closed, an audible click should be heard.

4.5.14.8: Vent Load-Lock Chamber

Vent the load-lock chamber by turned off the Load-Lock Vacuum-Pump power switch for venting load-lock chamber. This shut off the turbo and mechanical pumps and activated the turbo pump’s delayed vent valve.

4.5.14.8: Open Load-Lock Chamber

Once the load-lock chamber reached atmospheric pressure, aluminum load-lock cover is lifted and placed it face down on the four rubber pads on the table top.

4.5.14.9: Remove Sample Holder

Sample holder is removed carefully from the load-lock chamber.

4.5.14.10: Replace Cover

Aluminum load-lock cover is placed uniformly on the load-lock transfer port.

The process variables are given below in table.

Table 1

Process variables	values
Base pressure	$1 * 10^{-5}$mbar
RF power	125 W
Process pressure	$5.5 * 10^{-3}$mbar
Gas flow(Ar)	18.1 sccm
Gas flow(oxygen)	2.1 sccm
Deposition rate	0.4 A^0
Target to substance distance	8cm
Preheat temperature	100℃

4.6: Characterization techniques

4.6.1: Optical microscopy

The optical microscope analysis is carried out for surface morphology analysis of Ti6Al4V.It is a microscope which uses light source to capture the images. Initially the images were captured on photographic plate but modern developments lead to digital capturing of images.

4.6.2: Scanning Electron Microscopy

The scanning electron microscope (SEM) analysis is carried out for the surface morphology of Ti6Al4V. It uses high energy electron beams for capturing the images of surface sample by scanning it. Very high-resolution image details smaller than 1nm could be produced by scanning electron microscope .Closely spaced features could be examined at an ultra-high magnification by scanning electron microscope i.e. it is possible to produce high resolution

images by SEM. Scanning electron microscope could produce signals which contain information surface topography, composition and electrical conductivity. We used JEOL JSM-5300 microscope with acceleration voltage 15 kV for surface characterization of our samples. Samples were put in sample holder and then ushered inside the instrument. Finally, these samples were visualized under different magnifications.

4.6.3: Atomic Force Microscopy

Surface roughness of Ti6Al4V implant surface and TiO2 layer has been measured by atomic force microscope. AFM doesn't uses lenses or beam irradiations. It has a probe; the reaction of applied force on probe is used for 3D imaging of surface. It has very high resolution in fractions of nm.

4.6.4: Micro-Hardness Study

The micro hardness of Ti6Al4V surface and TiO2 layer has been measured by Vickers hardness method. LECO LM700 micro hardness tester has been used which is shown in figure. The machine can apply load from 1gf to1000gf.The test was carried out at 200gf for 12 second .10 readings of hardness were taken and averaged them for final micro hardness.

Chapter 5

Result and discussions

In this chapter, modifications in surface of Ti6Al4V dental implant due to thin film fabrication of titanium oxide are analyzed and discussed through characterization techniques. Optical microscope and scanning electron microscope are used for surface morphology analysis. AFM is used for roughness analysis and vicker's hardness tester is used for hardness analysis. Comparative analysis of roughness and hardness is carried out in MINITAB software.

5.1: Morphology Analysis

Microstructure of Ti6Al4V and thin films is analyzed by optical microscope and scanning electron microscope.

5.1.1: Optical micrographs

Optical micrographs were taken of the samples of Ti6Al4V before and after titanium oxide thin film deposition to analyze any change in morphology after the titanium oxide coating on surface of Ti6Al4V dental implant.

Figure 5 : optical micrograph of Ti6Al4V surface etched with tint reagent

Figure 6: optical micrograph of Ti6Al4V surface etched with kroll's reagent.

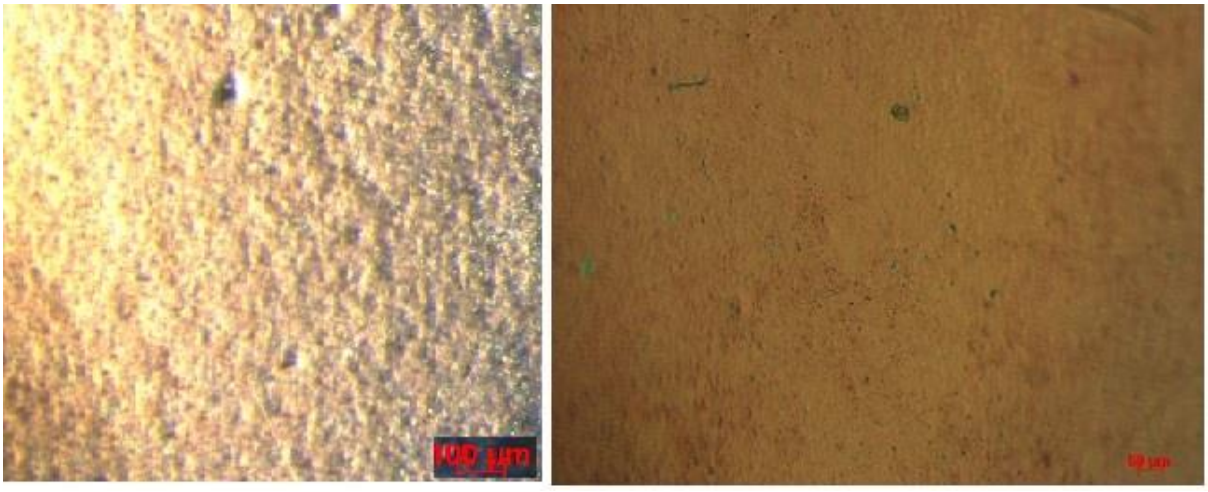

Figure 7: optical micrograph of thin film of titanium oxide deposited by magnetron sputtering.

Figure 5 shows the optical micrograph of Ti6Al4V etched with oxalic tint etch for 60 seconds. Tint etch reveals the color micrograph. Figure 6 shows the optical micrograph of Ti6Al4V etched with kroll's reagent for 45 seconds. Ti6Al4V is titanium alloy comprise of two phases alpha and beta. Alpha phase has hcp structure and beta phase has bcc structure. Ti has hcp structure at room temperature and phase transformation take place at 883C. This temperature is called beta transus temperature. If any beta stabilizer such as molybdenum and vanadium is added then we find below room temperature a combination of alpha and beta phase called α+β phase. Al and oxygen are alpha stabilizers, they stabilizes alpha phase of

alloy. Micrograph of Ti6Al4V shows the shiny alpha phase presented in α+β phase matrix. These alpha phases may be acicular, plate like and serrated in structure, very difficult to analyze in optical micrograph. Alpha phase has less hardness and more ductility than α+β phase. We can conclude that Ti6Al4V doesn't have uniform property at micron level.

Figure 7 shows the optical micrograph of thin film of titanium oxide deposited by magnetron sputtering. Micrograph shows more surface roughness.

5.1.2: Scanning Electron Microscopy (SEM)

SEM images of Ti6Al4V are taken before titanium oxide thin film deposition in different resolution and modes.Ti6Al4V is an Ti alloy preferably used in dental implant. It is a titanium alloy having Al and V as phase stabilizers. Al is alpha phase stabilizer where as vanadium is beta phase stabilizer .Titanium has HCP structured alpha phase below 883C. When any beta stabilizing element added it forms α+β phase at room temperature.Above 883C, it is bcc structured beta phase which is harder than alpha phase but has less ductility. In Figure 8**,** FE-SEM image of Ti6Al4V shows the α+β phase of alloy. In the α+ β phase alloy matrix, there are flakes of alpha phase. These flakes are shiny can be clearly seen in images. These flakes are formed due to gathering of alpha phase stabilizers. If beta phase stabilizer is in higher amount then beta flakes may be formed in alpha-beta phase alloy. These alpha phase flakes have lower hardness and strength but they have higher ductility than the alpha-beta phase in vicinity. Figure 9, shows the SEM micrograph of thin film of titanium oxide fabricated through reactive sputtering of Titanium and oxygen. The deposition of thin film on sample is almost continuous, uniform and crack free. Thin film is almost uniformly porous throughout.

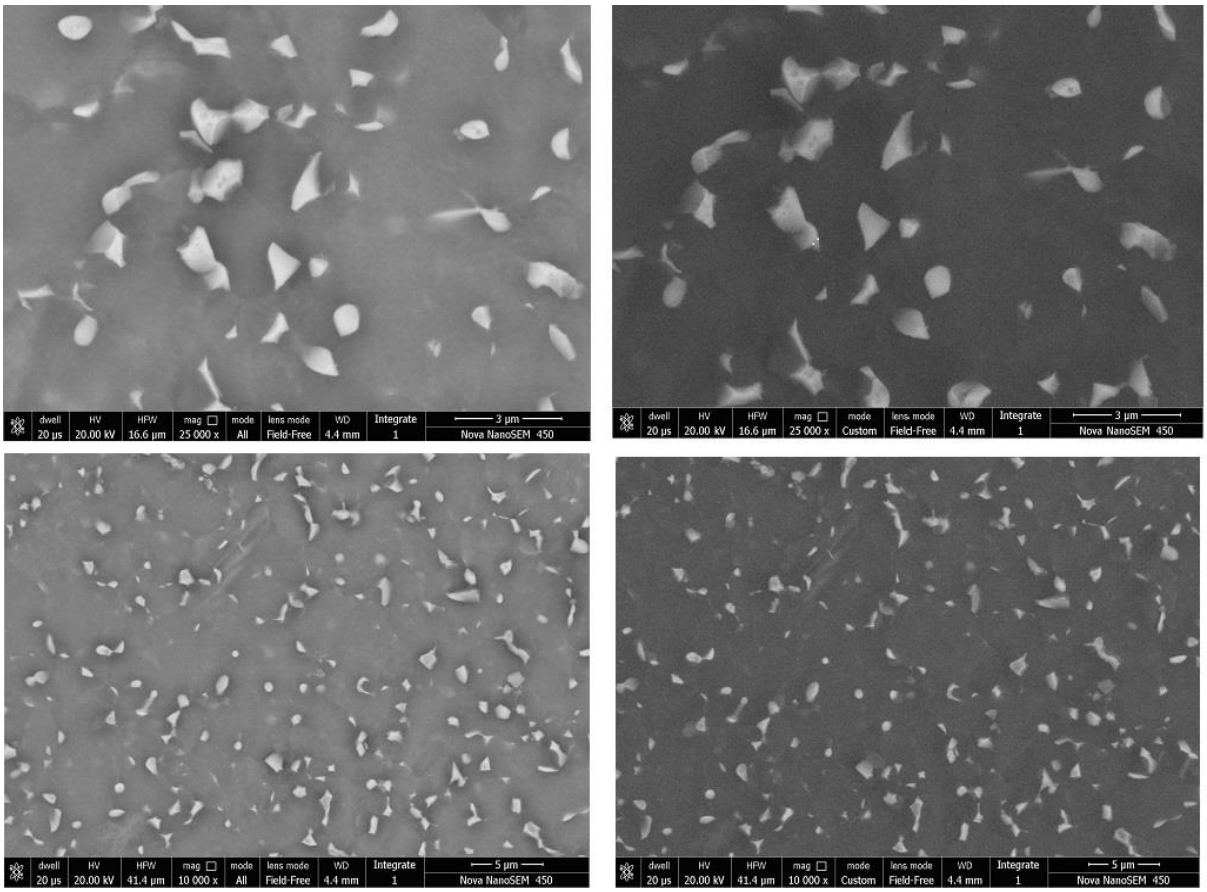

Figure 8: FE-SEM images of Ti6Al4V before thin film deposition.

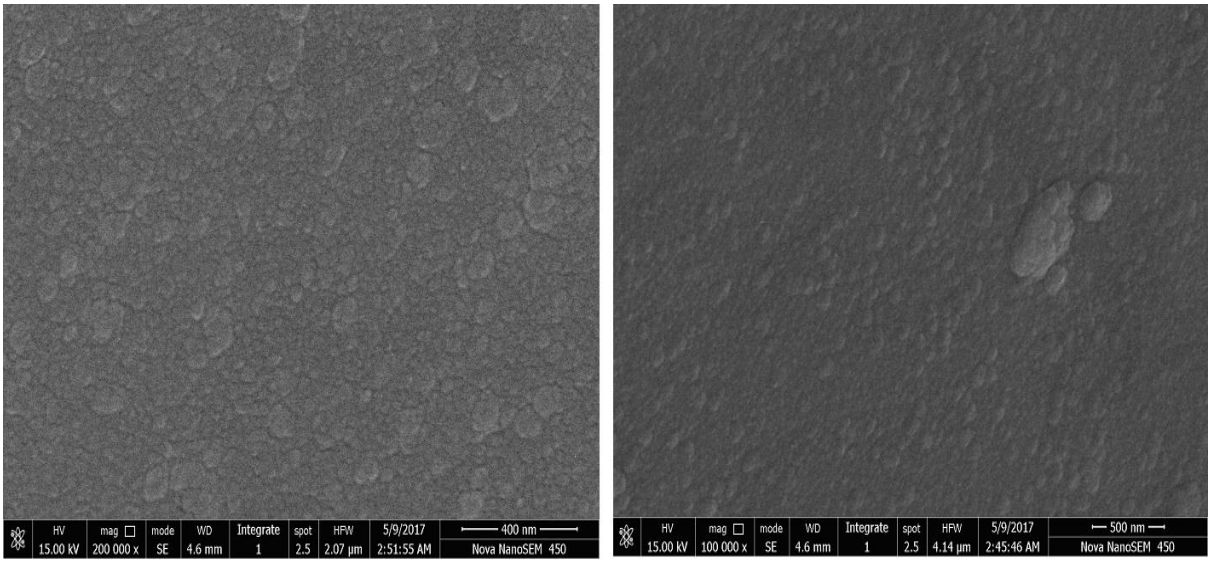

Figure 9: FE-SEM images of titanium oxide thin film deposited by sputtering

5.2 Atomic Force Microscopy (AFM)

Atomic force microscopy is carried out of Ti6Al4V dental implant and thin films deposited on them for the roughness study of surfaces. By the AFM micrographs, the roughness study is carried out of dental implant before film titanium oxide film deposition and after titanium oxide film deposition.

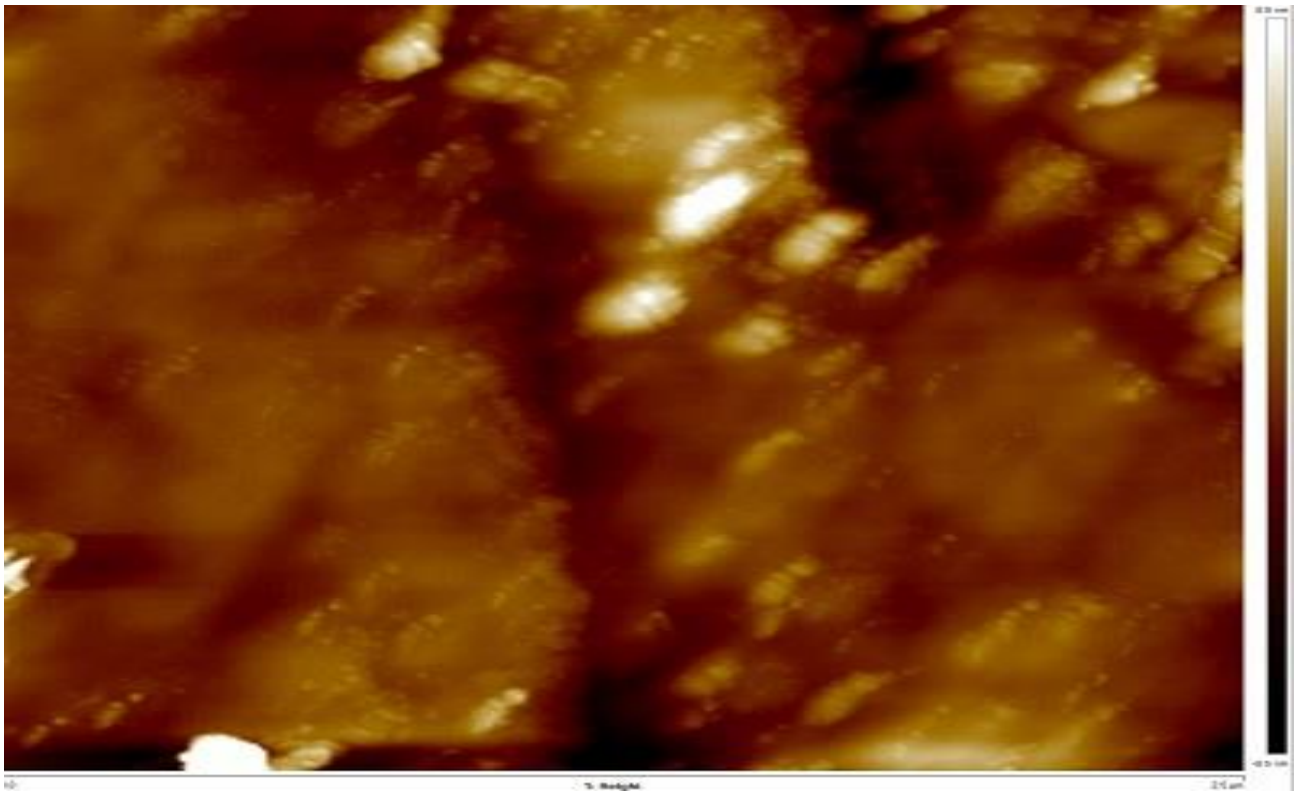

Figure 10: AFM 2D topography of Ti6Al4V

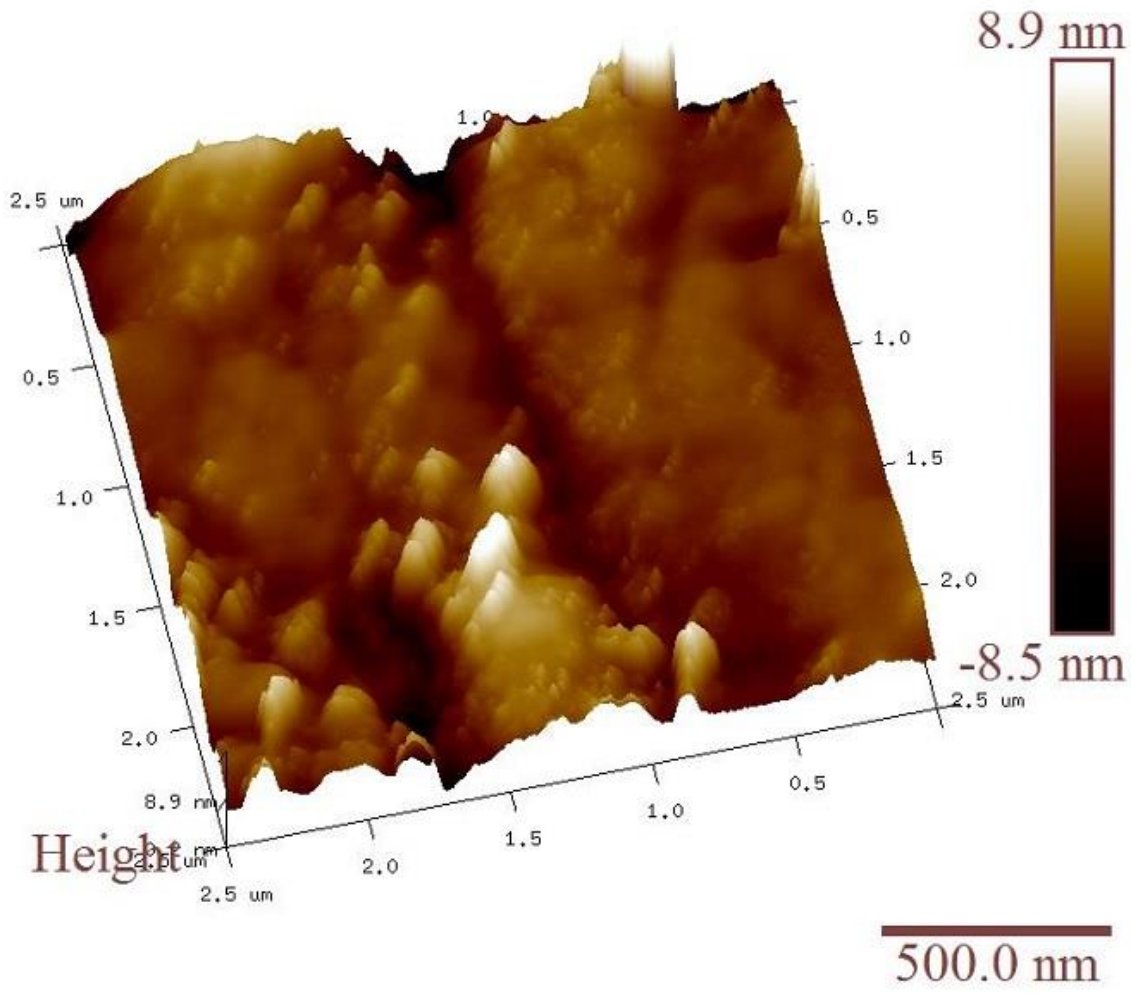

Figure 11: AFM 3D topography of Ti6Al4V

Atomic force microscopy is used to study the surface roughness of Ti6Al4V and titanium thin film deposited on sample. A comparative study is carried out. Figure 10 shows AFM 2D topographic image and Figure 11 shows AFM 3D topographic image of Ti6Al4V dental implant. Surface of Ti6Al4V dental implant have maximum roughness height is 41.3nm and arithmetic mean of roughness is 1.40 nm and root mean square roughness is 2.18 nm.

Table 2

Ti6Al4V		
R_{max}	**R_a**	**R_q**
41.3 nm	1.40 nm	2.18 nm

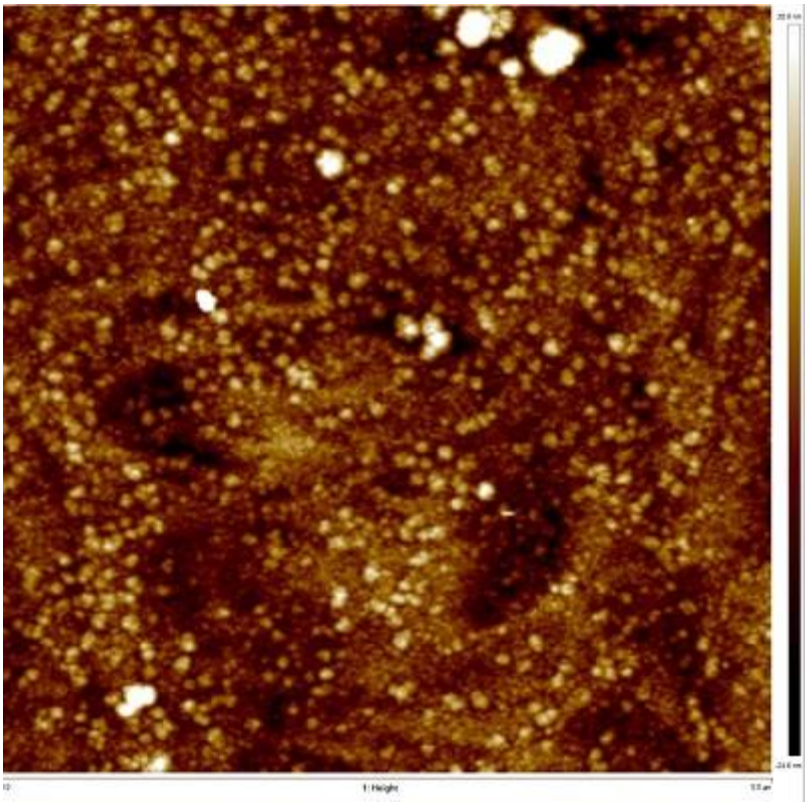

Figure 12: AFM 2D Topography of titanium oxide thin film fabricated by reactive magnetron sputtering

Figure 12 shows AFM 2D topographic image and Figure 13 shows AFM 3D topographic image of titanium oxide thin film fabricated by reactive magnetron sputtering of titanium and oxygen on Ti6Al4V dental implant. Surface of titanium oxide layer have maximum roughness height is 74.8 nm and arithmetic mean of roughness is 4.88 nm and root mean square roughness is 6.35 nm.

Table 3

Thin film of titanium oxide fabricated by reactive magnetron sputtering		
R_{max}	**R_a**	**R_q**
128nm	5.47 nm	7.44 nm

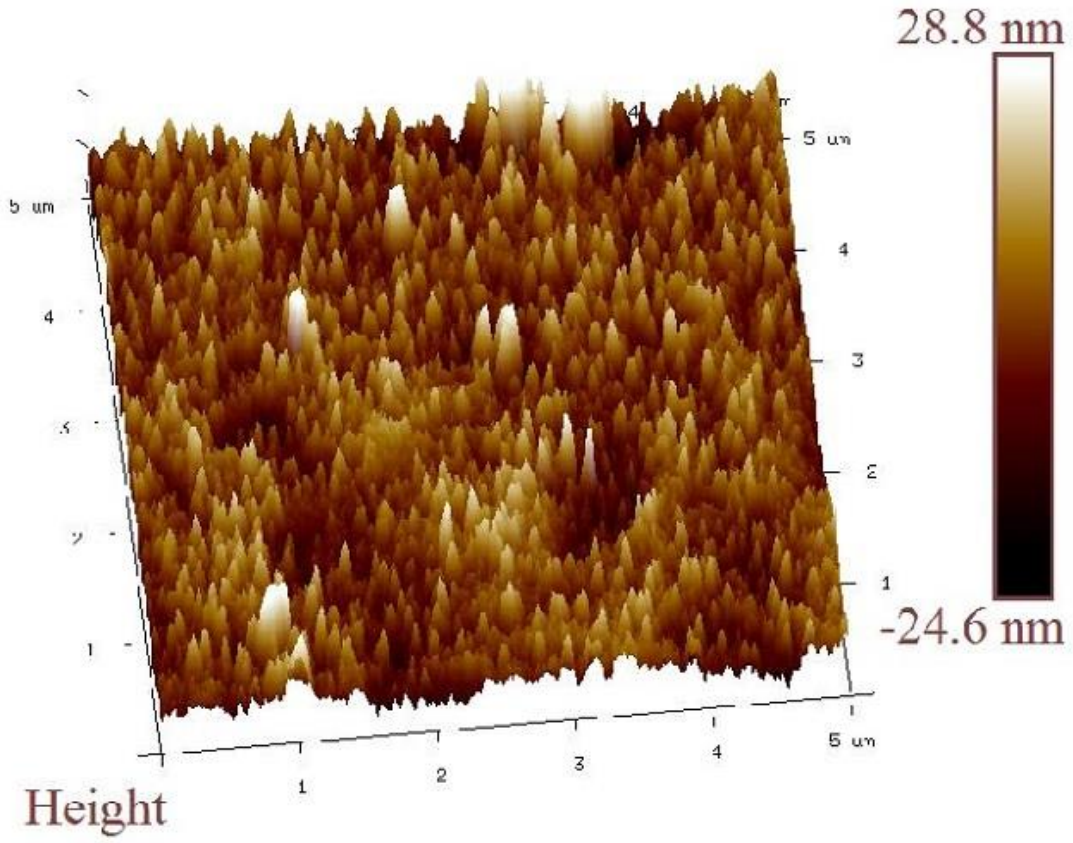

Figure 13: AFM 3D Topography of titanium oxide thin film fabricated by reactive magnetron sputtering

The comparative study of roughness can be done using stastics. Software minitab is used for stastic analysis of Ti6Al4V dental implant and his coatings.

Table 4

Sample	Average roughness (nm)
Ti6Al4V	1.40
Titanium oxide fabricated by sputtering	5.37

The comparative analysis of roughness is carried out in MINITAB through bar graphs.

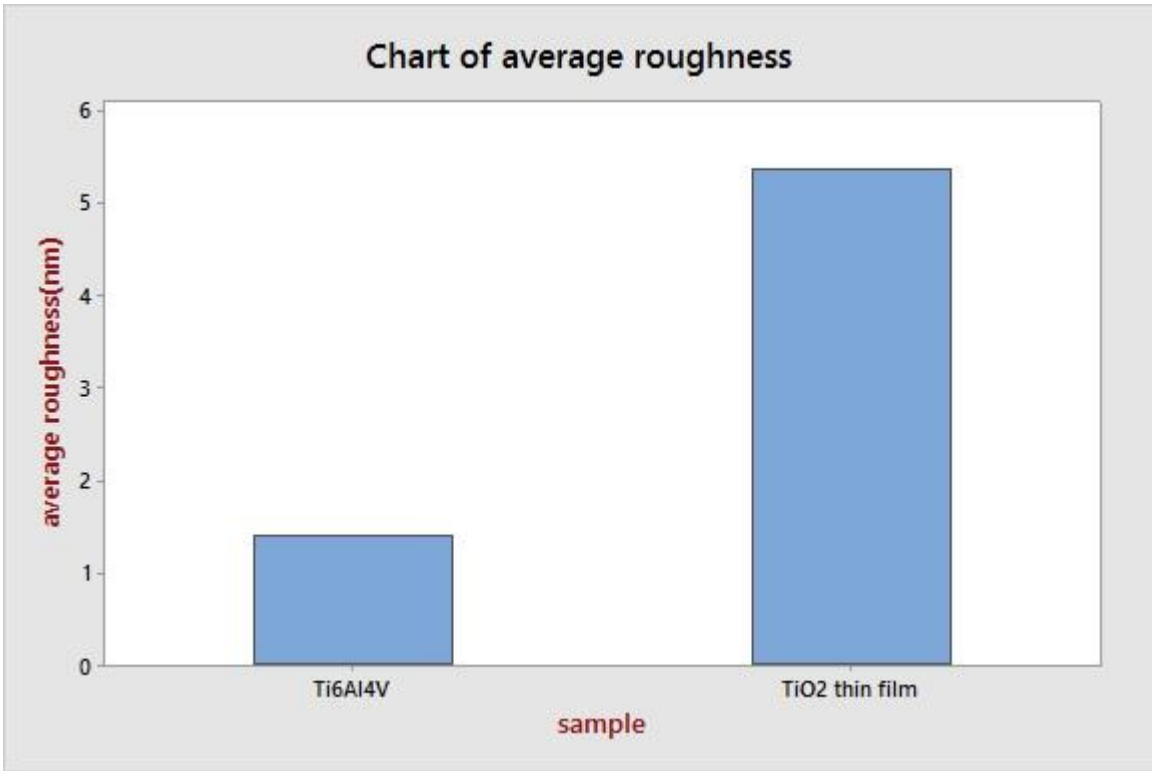

Figure 14: average roughness

In figure 14 average roughness is shown on y axis and sample is shown on x axis. Graph shows Ti6Al4V dental implant has minumum average roughness 1.40 nm. Titanium oxide coating fabricated by reactive sputtering has average roughness 5.37 nm.

Table 5

Sample	**Root mean square roughness (nm)**
Ti6Al4V	2.18
Titanium oxide fabricated by sputtering	7.44

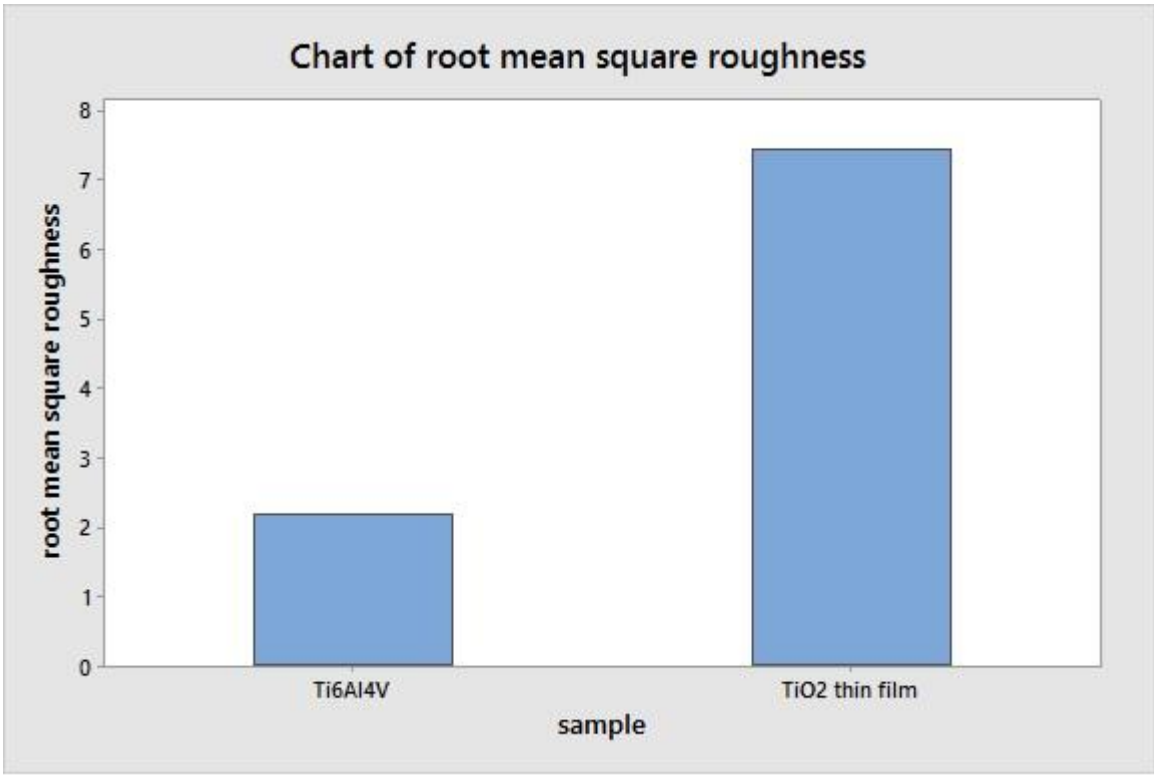

Figure 15: Root mean square roughness graph

In figure 15 rms roughness is shown on y axis and sample is shown on x axis. Graph shows Ti6Al4V dental implant has minumum rms roughness 2.18 nm. Titanium oxide coating fabricated by reactive sputtering has rms roughness 7.44 nm.

5.3: Micro Hardness Study

The micro-hardness of Ti6Al4V is measured before and after coating of titanium oxide by Vickers hardness tester.200gf is applied for 10 second in process of indentation. For hardness measurement, 10 readings are taken and average of them is obtained for each sample. Ti6Al4V has micro hardness 330 HV. Titanium oxide layer fabricated by reactive sputtering has micro hardness 380 HV and titanium oxide layer fabricated by oxidation of Ti in an electric furnace has micro hardness 350 HV.

Table 6

Sample	Micro hardness
Ti6Al4V	330 HV
Titanium oxide film fabricated by reactive sputtering	380 HV

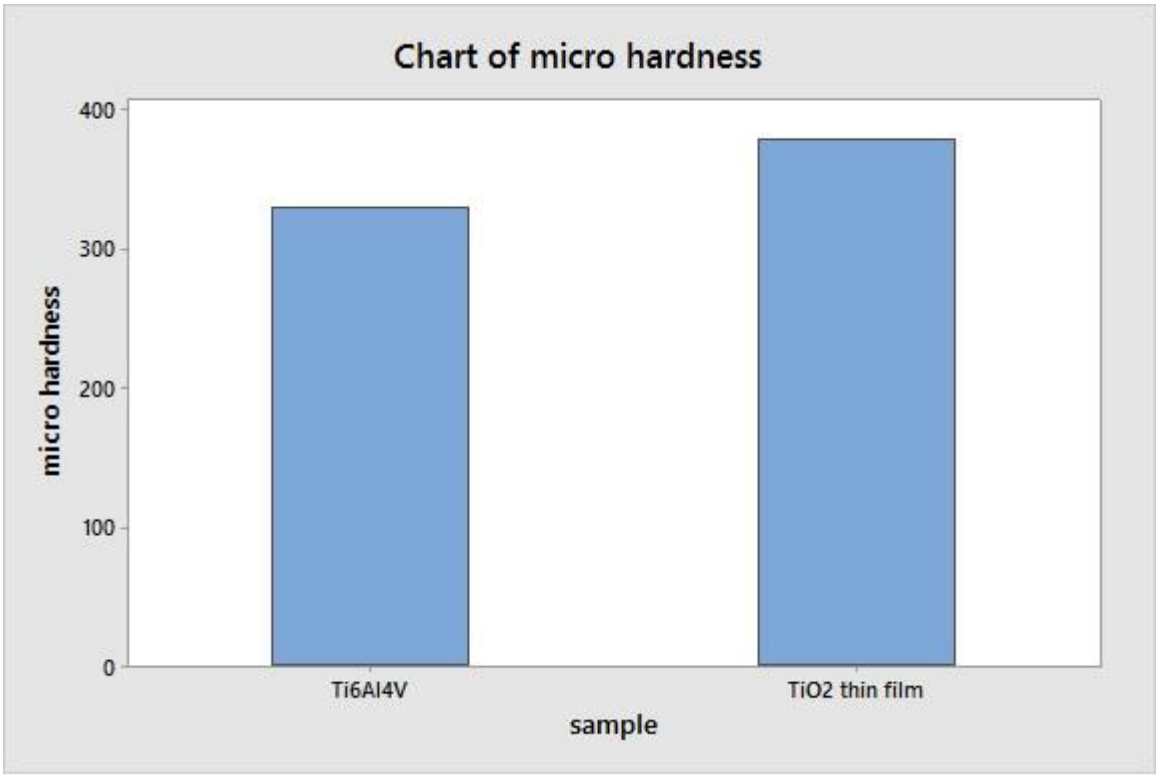

Figure 16: Micro hardness graph

Bar graph shows micro hardness of Ti6Al4V dental implant and thin films deposited on it. Titanium oxide film deposited by sputtering has highest micro hardness. Titanium oxide film deposited by thermal oxidation of titanium has less hardness than sputtered film.

Chapter 6

Conclusions and Future Scope

6.1 conclusions

1. Uniform, porous, continuous and crack free surface is obtained in titanium oxide layer fabricated by reactive sputtering of titanium and oxygen. This porous structure increases the surface area of implant. This porous structure is good for cell growth in vicinity of implant.
2. Titanium oxide has three crystalline structures, anatase, rutile and brookite phase. But usually exist in only two phases, brookite is very rare.
3. Titanium oxide layers have more roughness than the Ti6Al4V. This helps in better grip of implant. Higher roughness is good for osseointegration of dental implant. Rough surfaces are also good for biocompatibility than smooth surfaces.
4. Micro hardness test shows that titanium oxide thin film has more hardness than Ti6Al4V. Higher hardness implies higher wear resistance of implant. Hence the cracks generated due to the wear can be eliminated.

6.2 Future Scope

The aforementioned work has been performed on the material science aspects of Ti6Al4V, which may enhance the cell-implant interaction. Future studies could include 1) cell viability tests to understand the cellular behavior on each of the aforementioned modified surfaces, 2) x-ray photoelectron spectroscopy studies before and after thermal oxidation to obtain qualitative and quantitative analysis of the elements present on the substrates, and 3) grazing incidence x-ray diffraction investigation to understand the crystallinity of the Ti6Al4V substrates after thermal oxidation at various temperatures.

Literature studies have also shown that though TiO_2 is corrosion and wear resistant, over time, the dental and hip implants fail due to corrosion, wear, lack of osseointegration, and infection. Therefore, future studies need to be performed on the surface modification techniques which can provide surfaces that prevent corrosion and wear, improves osseointegration, and effectively 'fight' infection. In order to prevent wear and corrosion, robust and mechanically inert titanium nanotubes may need to be obtained so that Ti-based surfaces can withstand the tribology of the physiological movement and prevent corrosion due to the biological fluids of the body. For better future cell-implant interactions, titanium

nanotubes could be loaded with anti-inflammatory drugs, growth factor, or antibiotics to prevent inflammation, improve osseointegration, and minimize/eliminate infection, respectively.

References:

1. Geetha Manivasagam, et al., “Biomedical Implants: Corrosion and its Prevention - A Review”, Recent Patents on Corrosion Science, 2010, 4054(2), p. 15.
2. Becker, C.M.a.D.A.K., “Surgical guide for dental implant placement”,The Journal of Prosthetic Dentistry, 2000,83(2), p. 4.
3. Physical Vapor Deposition,Metal Deposition 2009 [cited 2012 15th october]; Department of Electrical and Computer Engineering:[Available from: http://www.cleanroom.byu.edu/metal.phtml.
4. N. Adya, M.a., T. Ravindranath, A. Mubeen, B. Saluja., “Corrosion in titanium dental implants: Literature review”, The Journal of Indian Prosthodontic Society, 2005, 5(3), p.6.
5. I., G., “Characteristics of metals used in implants”, Journal Endourol, 1997, 11(6), p. 6.
6. Total Hip Replacement 2011, Available from:http://orthoinfo.aaos.org/topic.cfm?topic=a00377.
7. Mikko Ritala, K.K., Antti Rahtu, Petri I. Raisanen, Markku Leskela, Timo Sajavaara, and Juhani Keinonen, “Atomic Layer Deposition of Oxide Thin Films with Metal Alkoxide as Oxygen Sources”, American Association for Advancement of Science, 2000,6,p.288.
8. Bhawani, C. Dentistry for Students: Dental Education Guide for Students. 2010; Available from: http://dentistryforstudents.com/parts-of-dental-implant/.
9. Albrektsson T, B.P., Hansson HA and Lindstrom J., “Osseo integrated titanium implants. Requirements for ensuring long-lasting, direct bone to implant anchorage in man”, Acta Orthop Scand, 1981, 52(2), p. 16.
10. Ashrafizadeh, A. and F. Ashrafizadeh, “Structural features and corrosion analysis of thermally oxidized titanium”, Journal of Alloy and Compound, 2009, 480(2), p. 849-852.
11. Youji Li., Wei Chen, Leiyong Li, “Preparation of titania-based multiple layer thin films with ordered-perforation pores and high photoelelctrocatalytic activity”, Materials Letters, 2011, 65(17-18), p. 2797-2799.
12. Grigal, I.P., et al., “Correlation between bioactivity and structural properties of titanium dioxide coatings grown by atomic layer deposition”, Applied Surface Science, 2012, 258(8), p. 3415-3419.

13. Bruni, S., et al., “Effects of surface treatment of Ti–6Al–4V titanium alloy on biocompatibility in cultured human umbilical vein endothelial cells”, Acta Biomaterialia, 2005, 1(2), p. 223-234.
14. George, S.M., “Atomic Layer Deposition: An Overview”, Chemical Reviews, 2010, 110(1), p. 21.
15. Mato Knez, A.K., Christina Wege, Ulrich Gösele, Holger Jeske, and Kornelius Nielsch, “Atomic Layer Deposition on Biological Macromolecules: Metal Oxide Coating of Tobacco Mosaic Virus and Ferritin”, Nano Letters, 2006, 6(6), p. 6.
16. T. Suntola, A.P., S. Lindfors, in U.S. Patent. 1983: U.S.
17. Zhengwen Li, A.R., and Roy G. Gordon, “Atomic Layer Deposition of Ultrathin Copper Metal Films from a Liquid Copper(I) Amidinate precursor”, Journal of The Electrochemical Society, 2006, 153(11), p. 8.
18. Song, X., D. Gopireddy, and C.G. Takoudis, “Characterization of titanium oxynitride films deposited by low pressure chemical vapor deposition using amide Ti precursor”, Thin Solid Films, 2008. 516(18), p. 6330-6335.
19. Leskela, M.R.a.M., “Atomic Layer deposition”, in Handbook of Thin Film Materials, H.S. Nalwa, Editor. 2002, Academic Press: Finland. p. 57.
20. Deal, B.E. and A.S. Grove, “General Relationship for the Thermal Oxidation of Silicon”, Journal of Applied Physics, 1965, 36(12), p. 3770-3778.
21. Masuda, H. and K. Fukuda, “Ordered Metal Nanohole Arrays Made by a Two-Step Replication of Honeycomb Structures of Anodic Alumina”, Science, 1995, 268(5216), p. 1466-1468.
22. Macak, J.M., H. Tsuchiya, and P. Schmuki, “High Aspect-Ratio TiO2 Nanotubes by Anodization of Titanium”, Angewandte Chemie International Edition, 2005, 44(14), p. 2100-2102.
23. Guang-zhong Li, Quan-ming Zhaon et al., “Fabrication, characterization and biocompatibility of TiO2 nanotubes via anodization of Ti6Al7Nb”, Composite Interfaces, 2016, 23(3), p. 223–230.
24. A. Biswas, L. Li et al., “Laser surface treatment of Ti-6Al-4V for bio-implant application”, Lasers in Engineering, 2007, 17(1-2), p. 59-73.
25. Damian Wojcieszak, Michalzur et al., “Mechanical and structural properties of titanium dioxide deposited by innovative magnetron sputtering process”, Materials Science-Poland, 2015, 33(3), p. 660-668.

26. Xiaomian Wu, Xiaochen Liu, Jie Wei, Jian Ma, Feng Deng, Shicheng Wei, "Nano-TiO2/PEEK bioactive composite as a bone substitute material: in vitro and in vivo studies**'',** International Journal of Nanomedicine,2012,7 p.1215-25.
27. Francisco López-Huerta, Blanca Cervantes et al., "Biocompatibility and Surface Properties of TiO2 Thin Films Deposited by DC Magnetron Sputtering", Materials 2014, 7, pp.4105-4117.
28. Vipin Chawla, R. Jayaganthan, A.K. Chawla, Ramesh Chandra, "Morphological study of magnetron sputtered Ti thin films on silicon substrate", Materials Chemistry and Physics, 2008,111, p. 414–418.
29. S. L. Sing, W. Y. Yeong et al., "Characterization of Titanium Lattice Structures Fabricated by Selective Laser Melting Using an Adapted Compressive Test Method", 2016, 56(5), p.735–748.
30. Justyna Kulczyk-Malecka, Peter J. Kelly et al., "Characterisation Studies of the Structure and Properties of As-Deposited and Annealed Pulsed Magnetron Sputtered Titania Coatings", Coatings 2013, 3, p. 166-176.
31. Ab. Benyoucef, Am. Benyoucef et al., "Structural and morphological study of TiO2 magnetron sputtering thin film for a photovoltaic application", Revue des Energies Renouvelables ICRESD-07 Tlemcen, 2007, 8, p. 61 – 65.
32. Ji Chon Lim and Kyu Jeong Song, "The Effect of Deposition Parameters on the Phase of TiO2 Films Grown by RF Magnetron Sputtering", Journal of the Korean Physical Society, 2014, 65(11), p. 1896-1902.
33. L Le Guéhennec, A Soueidan et al., "Surface treatments of titanium dental implants for rapid osseointegration", Academy of Dental Materials 2007, 23 (7), p.844-54.
34. Zhou Linxi, Yang Quanzhan et al., "Additive manufacturing technologies of porous metal implants", China Foundry, 2014, 11(4), p.322-331.
35. A. PAZO, E. SAIZ and A. P. TOMSIA, "Silicate Glass Coatings on Ti-Based Implants", Acta Mater. , 1998, 46(7), p. 2551-2558.
36. S. Sangeethl, S. Radhika Kathyayini et al., "Biocompatibility studies on Ti02 coated Ti surface", ICANMEET-20 13, p. 404-408.
37. Danuta Kaczmarek, Jaroslaw Domaradzki et al., "Hardness of Nano Crystalline TiO2 Thin Film", Journal of Nano Research Vol., 212, 18(19), p.195-200.
38. Claudia Fleck, Dietmar Eifler et al., "Corrosion, fatigue and corrosion fatigue behaviour of metal implant materials, especially titanium alloys", International Journal of Fatigue, 2010, 32(6), p.929-935.

39. M.A.L. Hernandez-Rodriguez , G.R. Contreras-Hernandez et al., “Finite element stress analysis of functionally graded dental implant of a premolar tooth”, Journal of Mechanical Science and Technology,2016,30(11),p.4916-4923.
40. Ken’ichi Yokoyamaa, Tetsuo Ichikawab et al., “Fracture mechanisms of retrieved titanium screw thread in dental implant”, Biomaterial, 2002, 23, p.2459-2465.
41. M. Gahlert, D. Burtscher et al., “Failure analysis of fractured dental zirconia implants”, Clin. Oral Impl. Res., 2012, 23, p. 287–293.
42. Keren Shemtov-Yona, Daniel Rittel et al., “Effect of Dental Implant Diameter on Fatigue Performance. Part I: Mechanical Behavior”, Clinical Implant Dentistry and Related Research, 2012, 35, p. 360-365.
43. Mohamed A. Hussein , Abdul Samad Mohammed et al., “Wear Characteristics of Metallic Biomaterials: A Review”, Materials 2015, *8*(5), p.2749-2768
44. Oguz Kayabasi, Emir Yuzbasioglu et al., “Stress analysis in dental prosthesis”, Computational Materials Science, 2010, 49(1), p.126-133.
45. A.Sliwa, L.A. Dobrzański, W. Kwaśny, M. Staszuk, “Simulation of the microhardness and internal stresses measurement of PVD coatings by use of FEM”, International Scientific Journal, 2010, 2(4), p.213-320.
46. Zhaohui Shan, Suresh K. Sitaraman, “Characterization of Mechanical Properties of Thin Films by Nanoindentation Technique and Finite Element Simulation”, IMECE, 2002, 39668(5), p.263-267.